Coastal Environmental Reseach Group
Department of Geology
Boston University
Boston, Massachusetts 02215

Technical Report No. 13
March 1989

# TIDAL HYDRAULICS, MORPHOLOGICAL CHANGES AND SEDIMENTATION TRENDS AT LITTLE RIVER INLET, MAINE

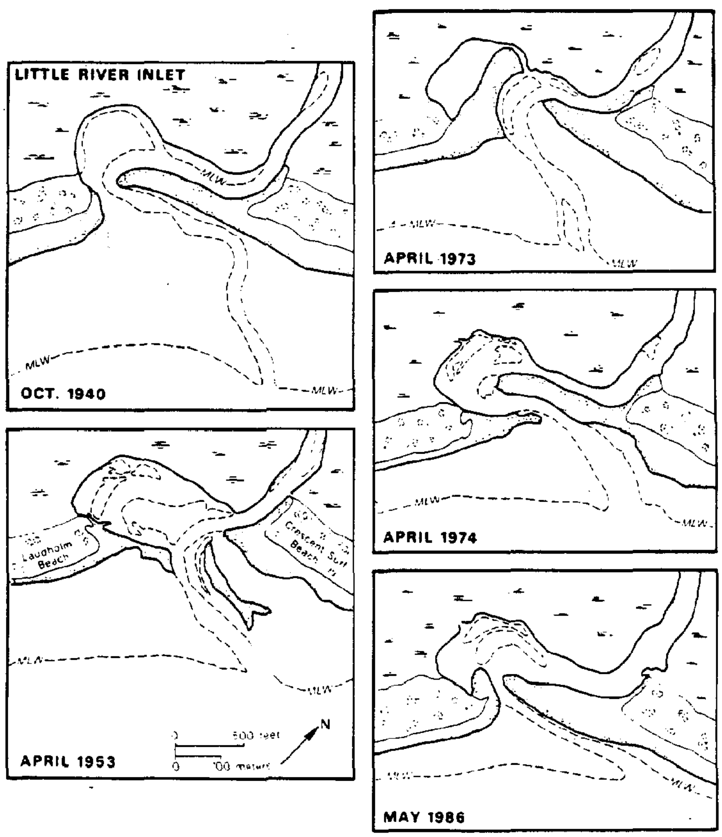




By Duncan M. FitzGerald and
Christopher G. Mariano

TIDAL HYDRAULICS, MORPHOLOGICAL CHANGES AND SEDIMENTATION

TRENDS AT LITTLE RIVER INLET, MAINE



Report For: NOAA's National Marine Sanctuary Program

Location: Wells Estuarine Research Reserve

March 1989

By: Duncan M. FitzGerald and Christopher G. Mariano
Coastal Environmental Research Group
Department of Geology
Boston University
Boston, MA 02215

TABLE OF CONTENTS

LIST OF FIGURES

## LIST OF TABLES

ACKNOWLEDGEMENTS

This project was supported by NOAA's National Marine Sanctuary Program. We wish to thank Jim List, manager of the Wells Estuarine Research Reserve for their assistance in this project. Steve Goodbred, Fred Abbuhl, Todd Montello, and J.B. Smith assisted with the fieldwork. Eliza McClennan, of the University Cartographic Services Lab drafted many of the figures. Steve Goodbred and Donna DeRosa edited and prepared the manuscript.

## ABSTRACT

Little River Inlet is one of the few tidal inlets along the southern Maine coast that is neither stabilized by jetties or natural bedrock outcrops. However, eroded glacial deposits (gravel lag) beneath the barrier sands may provide some underlying control of the inlet's position. The origin of the inlet is closely related to the presence of the Merriland River and Branch Brook which join to form the Little River. The flood plain associated with this fluvial system provided the topographically low areas that were flooded during the recent transgression. Today these regions are the extensive marsh systems found in the backbarrier of Laudholm and Crescent Surf Beaches that drain through Little River Inlet.

While the backbarrier system of Little River Inlet is relatively large, most of the surface is supratidal consisting of S. patens marsh (96%). Consequently, the bay tidal prism is small as compared to the extent of the backbarrier area, and the inlet channel has a small (22 $m^2$) equilibrium cross sectional area. Freshwater discharge at the inlet is greatest during large precipitation events, particularly during spring freshets. Freshwater comprises 11% of the inlet tidal prism of $2.8 \times 10^5$ $m^3$.

The inlet has been sited in its same approximate position

during the past two centuries as indicated by the oldest historical map of the region. An analysis of aerial photographs over the past 50 years shows that while the inlet has undergone slight northeast and southwest movement (< 200 m), there has been no net migration of the inlet. The sequential photographs also reveal that sand deposition in the form of recurved spits and flood-tidal deltas has caused some filling behind Laudholm Beach in the backbarrier region.

A sill exists 50 m seaward of the inlet throat and has an elevation of 1.21 m above mean low water. The sill strongly influences inlet hydraulics by causing a truncation of the tidal wave. The sill serves to extend the period of the ebb cycle while shortening the flood cycle, producing a flood dominated inlet channel. Tidal ranges in the backbarrier equal the ocean high tide level minus the sill height and low tide water depth over the sill.

## INTRODUCTION

Little River Inlet is situated between the double spit system of Crescent Surf Beach to the north and Laudholm Beach to the south, and is one of the few tidal inlets in Maine that is unstructured and not pinned next to bedrock (Figs. 1 and 2). Little River, which forms from the confluence of Branch Brook and the Merriland River, comprises the northeast boundary of the Wells National Estuarine Research Reserve. Although the inlet has an extensive backbarrier area, its channel system is relatively narrow and shallow due to the small tidal prism that is exchanged between the ocean and bay. The inlet mouth is subject to small migrations and morphologic changes which usually can be attributed to storm processes and accretionary recovery periods.

The small size of the Little River Inlet makes it an ideal location to study inlet hydraulics and sand transport patterns. The objective of this investigation was to document the current regime at the inlet and explain the ebb or flood dominance of the main channel in terms of the inlet hydraulics. A second goal of the study was to define the historical changes that have occurred to the area and to see how these changes correlate with present sand transport processes.

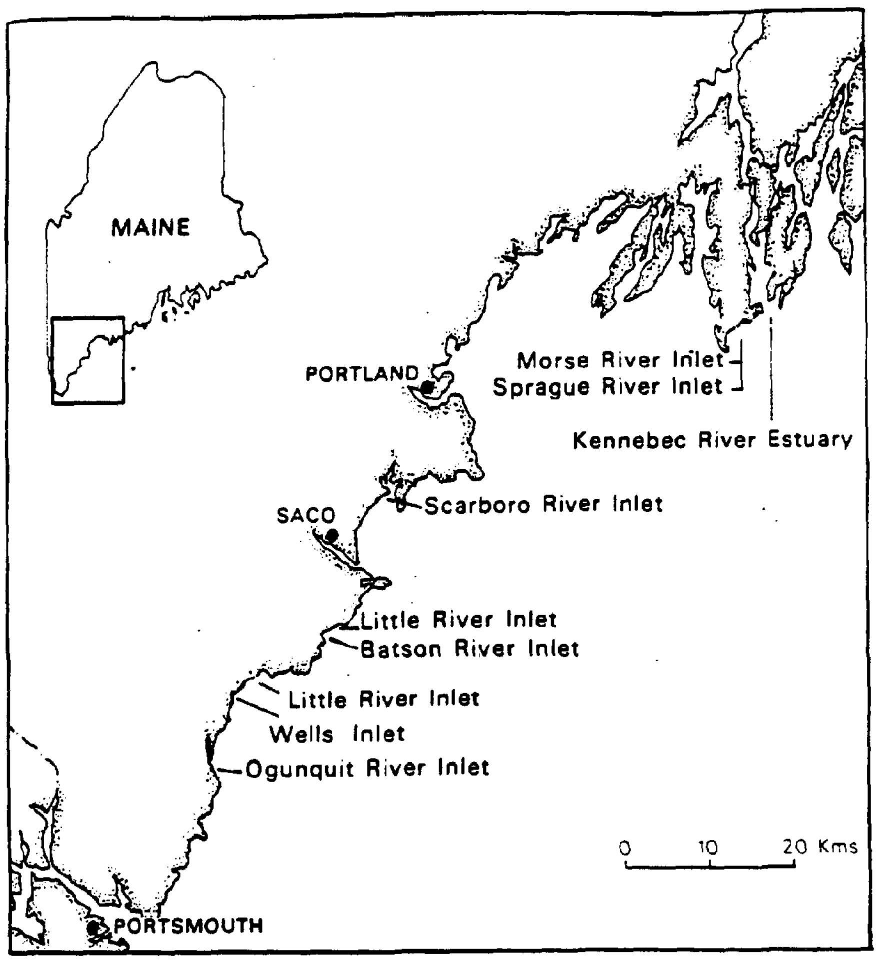


Figure 1. Location of Wells and Little River Inlets and other inlets studied along the coast of Maine.

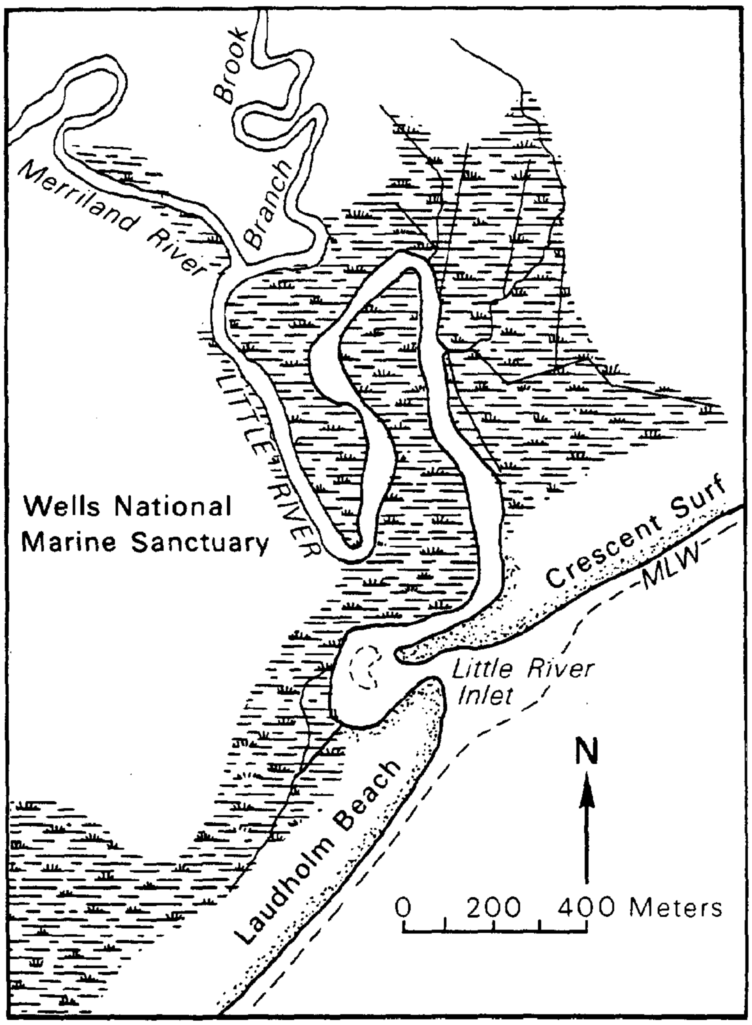


Figure 2. Map of study area.

# PHYSICAL ENVIRONMENT

## Location and Physiography

Little River Inlet is located along the southern coast of Maine approximately 45 km south of Portland Harbor and 30 km north of the Pisqataqua River (Figs. 1 and 2). The bedrock geology of this region is characterized by a narrow belt of metasedimentary/metavolcanic rocks that have been intruded by plutons of various age (Devonian through Triassic). The coastline has developed parallel to the regional structural trend and is dominated by bedrock headlands and intervening sand embayment. Timson (1977) in his physiographic classification of Maine's coast has termed this section the Arcuate Embayment shoreline.

The barriers of this compartment consist of relatively narrow spits that are backed by extensive marsh systems. The barrier complex of Goose Rocks with its seaward prograding beach ridges is a major exception to this trend. Tidal inlets are located at the end of many of these spits and are usually anchored next to bedrock headlands. The Saco River is the only major river along this stretch of shoreline although numerous small streams discharge into the area.

The marsh system behind Little River Inlet consists of supratidal marsh, intertidal flats and a network of incising tidal creeks (Fig. 3). The backbarrier covers an area of

Figure 3. Backbarrier setting of Little River Inlet.

2.51 $km^2$, of which 0.24 $km^2$ is open water, 0.06 $km^2$ intertidal sand and mud flats, and 2.21 $km^2$ *Spartina patens* salt marsh (Fig. 4). Despite the large size of its backbarrier, Little River Inlet has a small tidal prism and a small equilibrium channel cross section. This is due to the bay being filled with *Spartina* marsh, a quality that is characteristic of many tidal inlets in Maine. The reason for the large percentage of the backbarrier at a supratidal elevation is not known, however, it may be related to a high rate of peat production or initial sedimentation in the bay.

## Estuarine Conditions

Little River Inlet forms at the juncture of Branch Brook and the Merriland River. Although the width of Little River Inlet (w = 27 m) is considerably smaller than Wells Inlet to the south (w = 122 m), its drainage area (84 $km^2$) is over twice as large (Fig. 5). The mean annual discharge of Little River is estimated to be 1.4 $m^3$/sec over a half cycle (6.2 hrs). Thus, unlike Wells Inlet, the freshwater contribution of Little River comprises a relatively large percentage (11%) of the bay tidal prism ($2.8 \times 10^5 m^3$). The freshwater discharge at the inlet is most noticeable at the end of the ebb cycle when the channel waters are brackish to almost fresh on occasion. During winter cold snaps, the backbarrier channel completely freezes over.

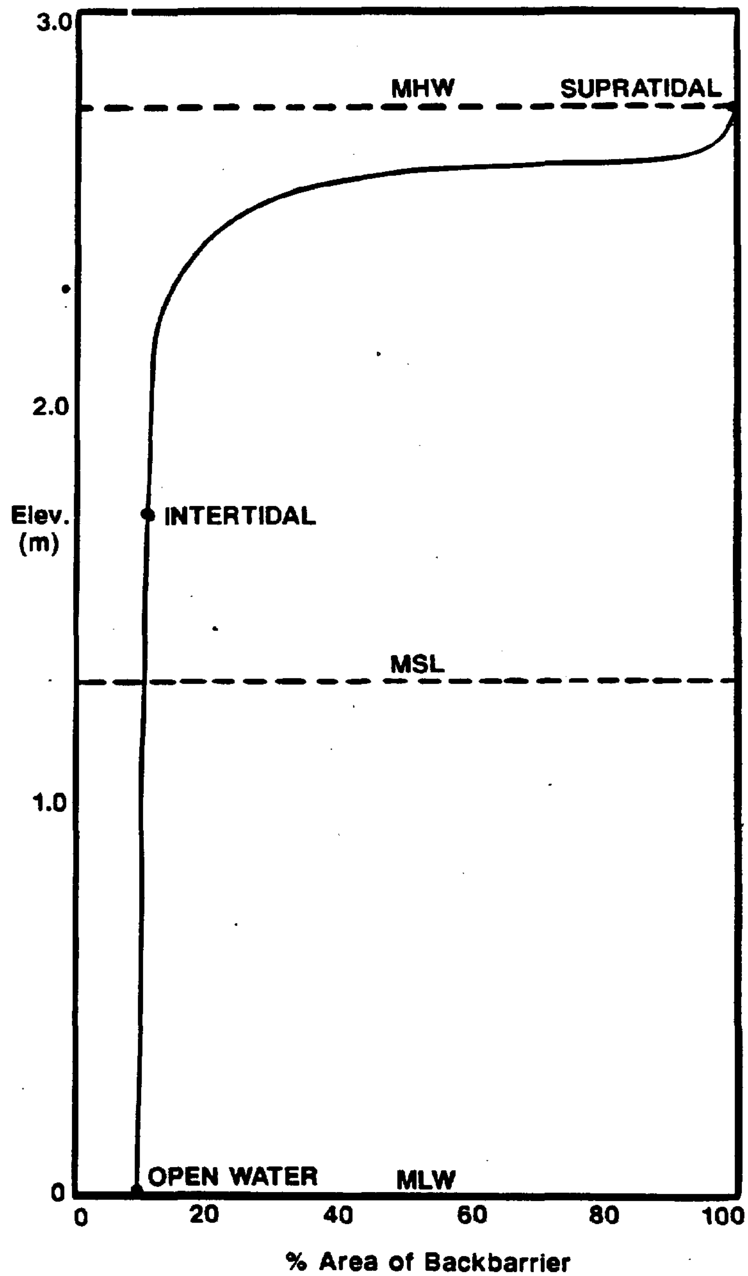


Figure 4. Hypsometric curve of Little River Inlet backbarrier. Like Wells Inlet, most of the backbarrier consists of supratidal *Spartina patens* salt marsh.

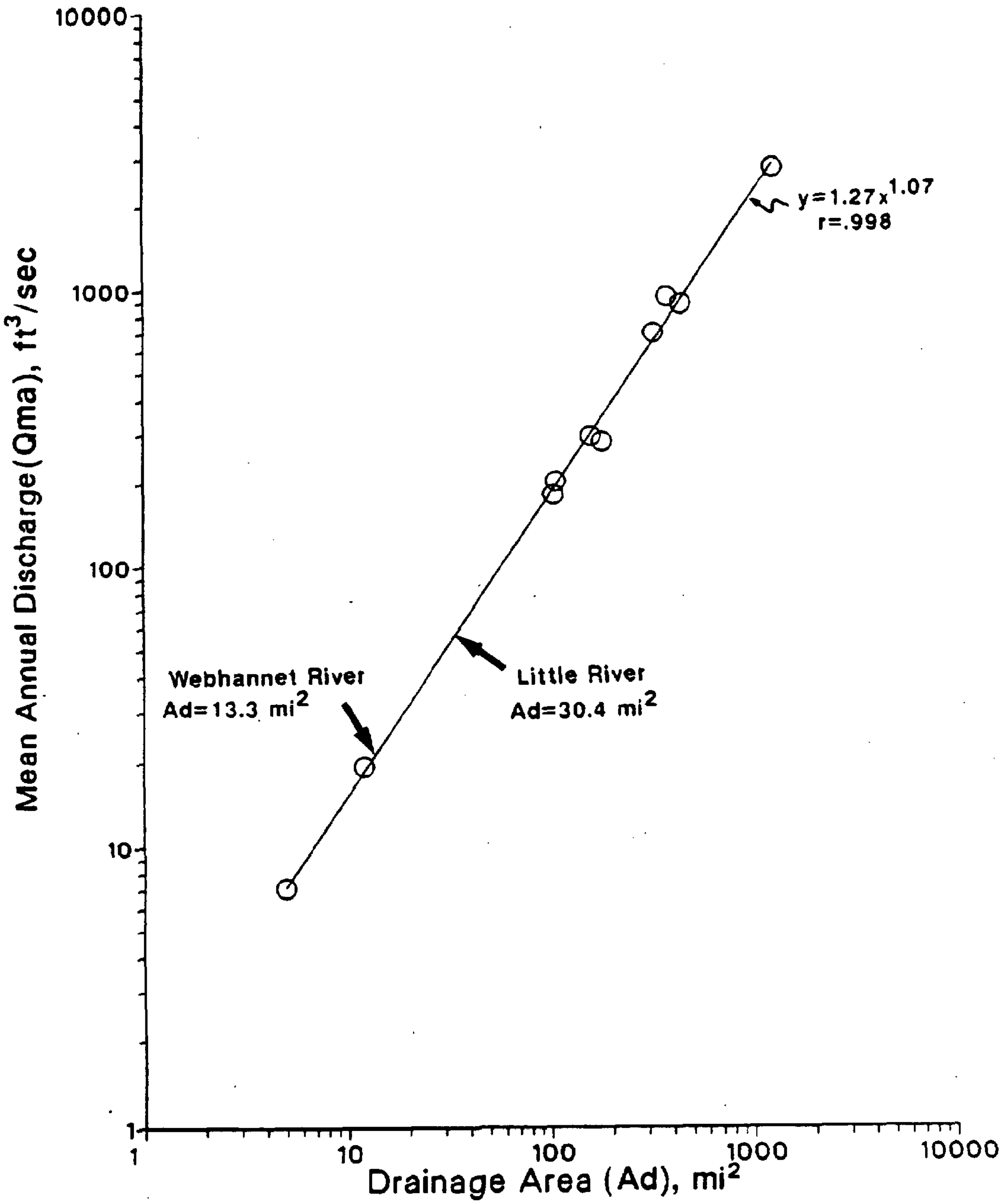


Figure 5. Plot of drainage area versus mean annual discharge for several rivers in east-central York County. Taken from D'Amore (1983).

## Wind Regime

The winds for this region are known from data collected at Bailey Point in Wiscasset and at Sequin Island Lighthouse (Figs. 6 and 7; Nelson and Fink, 1978 and Fink et al., in press). Both data sets are fairly consistent indicating the same seasonal trends. The prevailing winds blow from the western half of the compass with the months of May through September showing the greatest periods of calm. During the winter months the region is affected by strong wind activity from both extratropical storms and the passage of high pressure systems through the area. October and April are transitional months with strong east to northeast winds superimposed on either the increasing or decreasing intensity of the prevailing westerly pattern.

The dominant winds are from the northeast and are associated with extratropical storms that track east of the Gulf of Maine. Strong winds also blow from the northwest and southwesterly directions (Figs. 6 and 7). Because these winds are prevailing winds and at times are quite strong, they exert the greatest control on deviations from the astronomically induced tidal ranges. In turn, this influences tidal prism and tidal current conditions at inlets. The winds accompanying northeast storms not only affect tidal processes at inlets, but also significantly increase the transport of sand along the beaches to inlets.

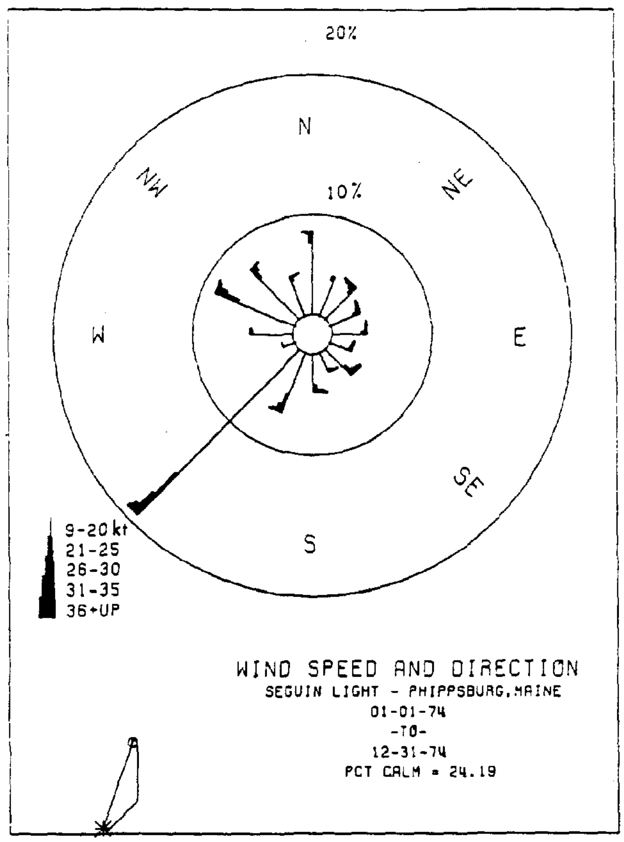


Figure 6. Wind rose for the southern Maine coast. Data collected at Baily Point, Wiscasset, ME (from Nelson and Fink, 1978). The dominant wind is from the northeast and is associated with northeast storms. The prevailing winds during the fall and winter are from the northwest and during the spring and summer they are from the southwest.

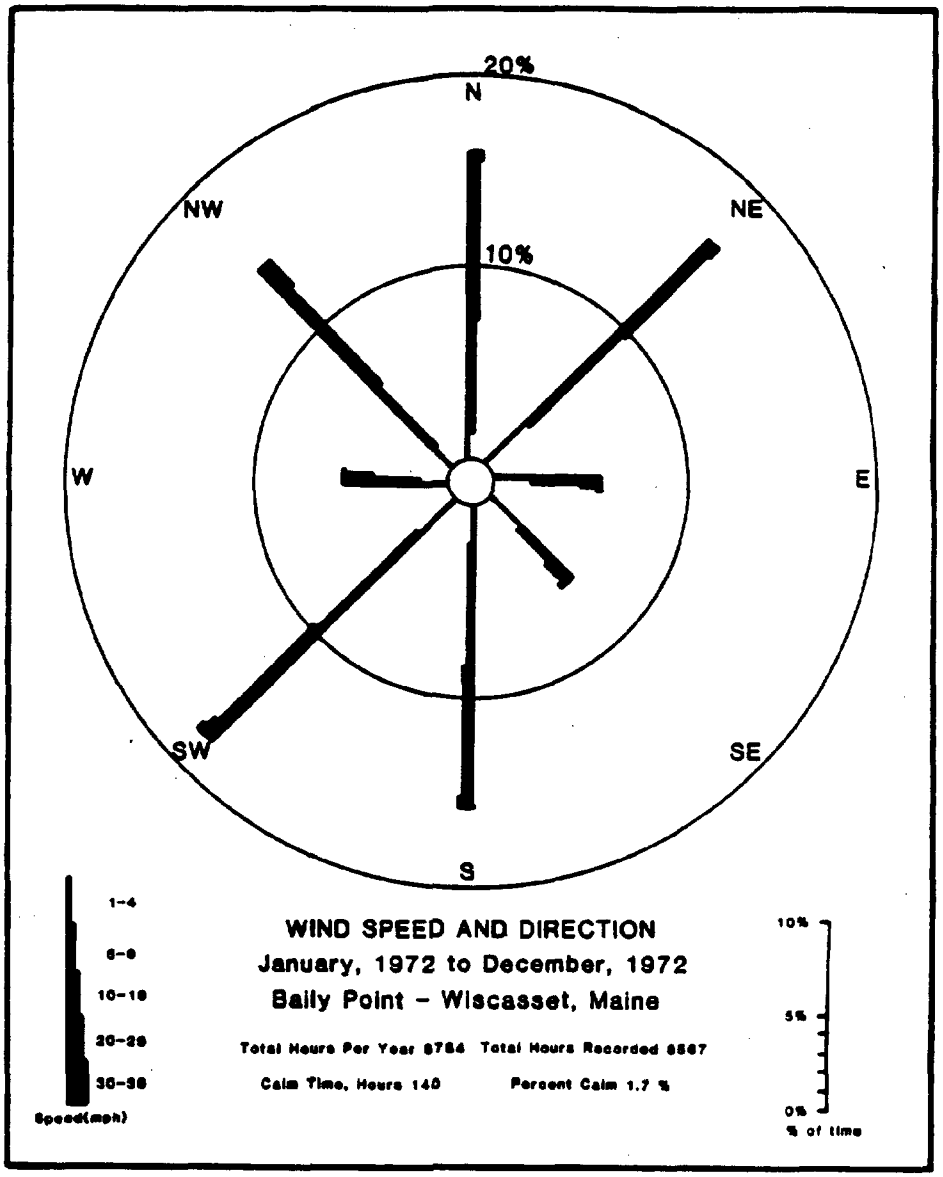


Figure 7. 1974 annual wind rose and resultant wind vector diagram for Sequin Island, ME based on hourly readings (from Fink et al.; in press).

## Wave Energy

Wave roses have been compiled by the U.S. Army Corps of Engineers for Penobscot Bay for deepwater conditions (Fig. 8; U.S. Army Corps of Engineers, 1957) and for 16 stations along the Maine coast for shallow water conditions (Figs. 9 and 10; Jensen, 1983). These analyses were based on hindcast studies using three years and 20 years of wind data, respectively. The deepwater wave rose shows that waves over 1.5 m come predominantly from the east and northeast and that waves over 4 m come only from these directions, reflecting the influence of northeast storm winds over a long fetch. The average deepwater wave height at the Penobscot Bay site is 90 cm.

Farrell et al. (1971) summarized data for northeast storms and demonstrated that the average storm wave approach is 79 degrees having breaker heights between 0.9 and 1.4 m and periods of 6 to 8 seconds. They also showed that low pressure systems that track inland produce significant storm waves from the southeast with an average approach direction of 157.5 degrees. Southeasters generally have lower wind velocities than northeast storms, have a shorter duration and produce smaller storm surges, smaller wave heights and shorter wave periods.

In shallow waters (depth = 10 m), Jensen's (1983) wave

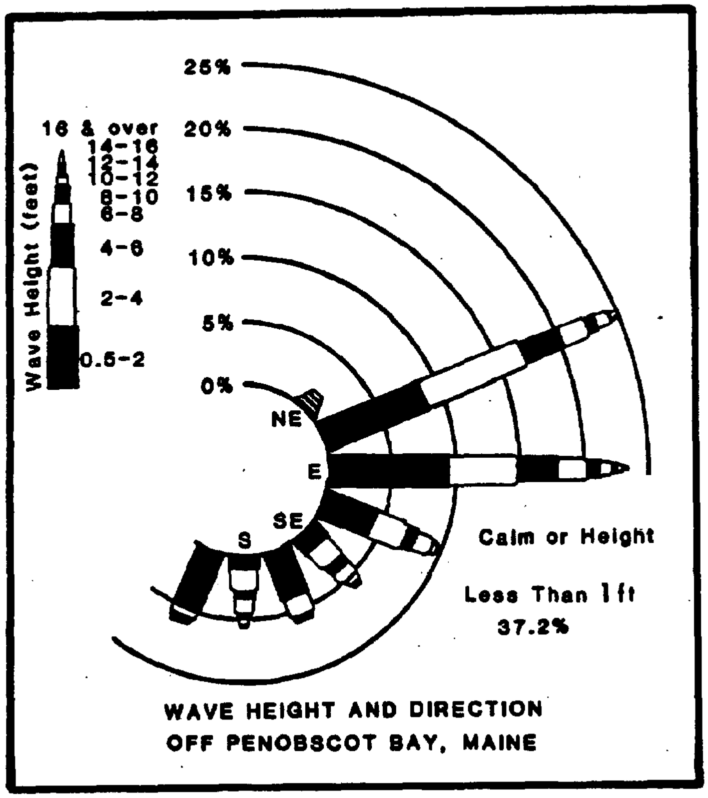


Figure 8. Wave diagram of deepwater wave heights hindcasted from three years of wind observations (1947-1950) for the region offshore of Penobscot Bay (from U.S. Army Corps of Engr., 1957).

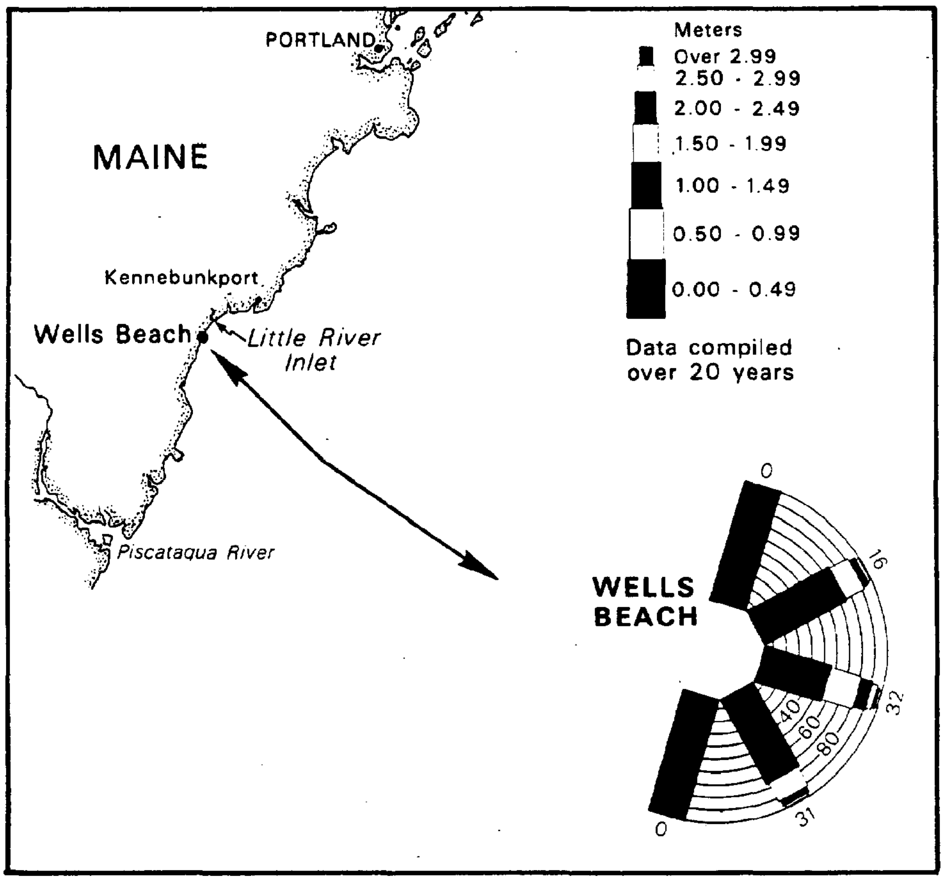


Figure 9. Nearshore (10m) wave diagram for the Wells region (data from Jensen, 1983).

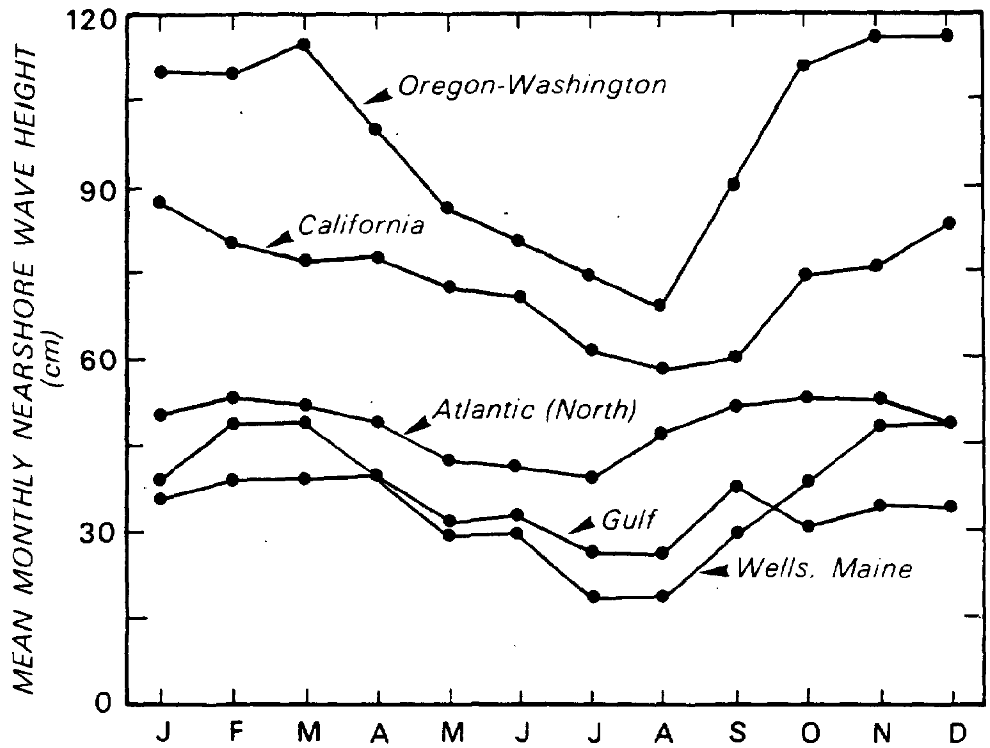


Figure 10. Monthly mean nearshore wave heights for various locations throughout the United States (Richardson, 1977) including the Wells area of Maine (Jensen, 1983).

data set for the Wells area shows that the dominant wave approach is from the eastsoutheast (Fig. 9). Average monthly wave heights are greatest during February, March, November, and December with a mean height of 50 cm. The lowest waves occur during July and August with an average height of 20 cm (Fig. 10). This region has slightly lower wave energy than the northern Atlantic coast and slightly greater energy than the Gulf of Mexico.

## Tides

Tides in the Gulf of Maine are primarily driven by semidiurnal deepwater tides in the North Atlantic. At the edge of the continental shelf, the tide is 0.84 m (Fig. 11) and occurs approximately 12 hours after the moon's transit at Greenwich, England (Redfield, 1980). Tidal amplification, due to close correspondence between the lunar $M_2$ component and the natural resonant frequency of the Gulf of Maine (Garrett, 1972; Greenberg, 1979), increases the mean tidal range to 2.7 m along Maine's southern coast. During spring tide conditions, the range increases to 3.5 m. In the coastal classification scheme of Hayes (1979) and Nummedal and Fischer (1978), a tidal range of this magnitude and an average deepwater wave height of 90 cm places southern Maine inlets in a tide dominated-mixed energy regime (Fig. 12).

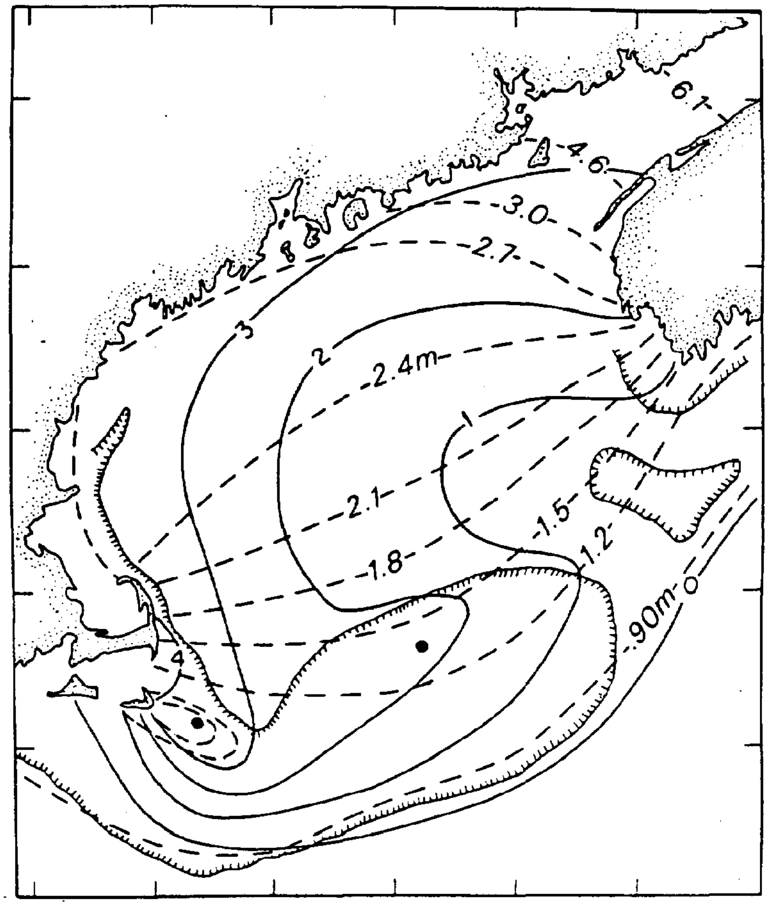


Figure 11. Corange and cotide lines for the Gulf of Maine amphidromic system. Lines of equal range are dashed and the lines of synchronous high tides (hours lag behind continental shelf tide) are solid (from Redfield, 1980).

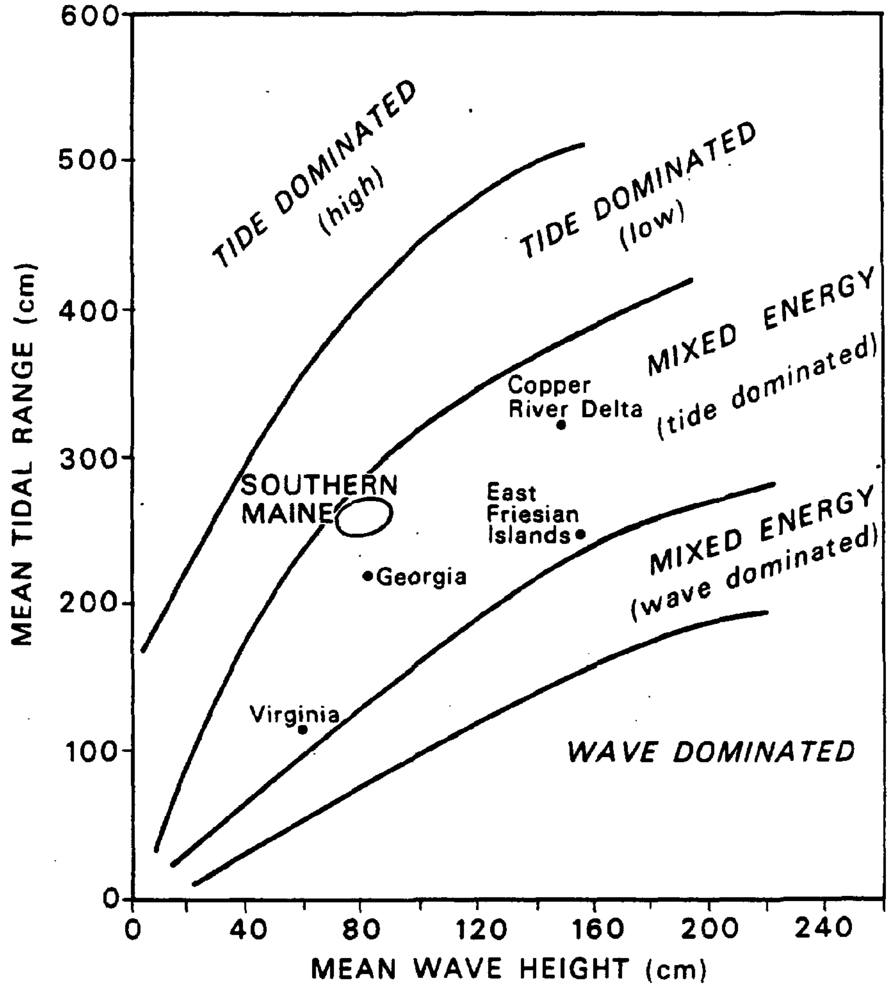


Figure 12. Shoreline classification based on tidal range and average deepwater wave height (Hayes, 1979; Nummedal and Fischer, 1978). Little River Inlet plots in the mixed energy, tide-dominated setting.

## Longshore Sediment Transport

The longshore movement of sand on the coast has been calculated by Byrne and Zeigler (1977) from the volume of sand trapped on both sides of the jetties and the amount of sand carried into the harbor. They estimated that 27,000 to 42,000 $m^3$ of sand was moving north and 13,000 to 27,000 $m^3$ of sand was moving south, indicating net transport of about 14,000 $m^3$ of sand to the north. This estimate is consistent with the wave refraction analysis and visual observations which showed that a greater percentage of waves approach the inlet from the south than from the north (Byrne and Zeigler, 1977).

# METHODS

## Introduction

The field portion of this project spanned 16 months from July 1987 to October 1988. During this period the collection of field data involved studies designed to determine the hydraulic and sedimentological character of the inlet. Tidal current data was needed to establish the flood or ebb dominance of various portions of the inlet channel and harborage area. This information also aided the tidal characterization of the inlet with regards to the distribution of tidal currents, their time and velocity asymmetry, and their magnitudes.

Sediment samples were gathered throughout the inlet region in hopes that grain size distributions would aid in establishing transport pathways. Due to the small sample size and wide variability of sediment sizes at the inlet, this study was only partially successful. Bathymetric profiles taken at the inlet were taken to determine if the inlet was migrating or undergoing any significant morphological changes.

## Hydrographies

Current velocities and tidal heights were monitored at five stations throughout Little River Inlet in order to establish the hydraulic character of the inlet. Velocities and directions were recorded using a Marsh-McBirney electromagnetic suspended flow meter. During the hydrographies, stations were monitored every 40 minutes over a complete 13 hour tidal cycle. Readings were taken through the water column and then depth averaged. The hydrographies were conducted during spring, mean and neap tidal conditions. Tidal elevations, during the velocity studies, were measured from a tide staff which was located 100 m landward of the inlet throat. The staff was read every 20 minutes.

## Channel Surveys

Several cross sectional profiles were taken throughout Little River Inlet to document channel morphology and to monitor erosional/depositional changes and migrational trends. During a twelve month period five of the profiles seaward of the inlet throat were surveyed a total of nine times. This work was completed using a standard beach profile technique. In addition, a longitudinal profile was made from the flood-tidal delta down the axis of the channel to determine the hydraulic gradient of the inlet.

## Sediment Sampling

Surface sediment samples were collected throughout Little River Inlet to supplement the hydraulic and bedform data in establishing tidal flow patterns at the inlet. Sieve analysis of the sediment samples was done to determine grain size statistics. A total of 35 samples were taken from the mouth of the inlet to the convergence of Branch Brook and the Merriland River. The samples were collected by core tube in the shallow portions of the channel and by grab sampler in the deeper sections.

Sediment samples were washed and treated with dilute hydrochloric acid solution to remove shell fragments. They were then rewashed, dried and sieved through screens using a range of mesh sizes from -2.0 to 4.0 phi (4.0 to .0625 mm) at 0.5 phi (0.71 mm) intervals. Graphic statistical mean grain size and sorting were calculated using the procedure outlined by Folk (1968).

## EVOLUTION

### Holocene

The development of the Little River estuary has involved a complex set of processes, including glacial erosion and deposition, isostatic and eustatic sea level changes, and Holocene sediment reworking operating within a bedrock framework. McIntire and Morgan (1964), in a study of beaches between Cape Ann, MA and Cape Porpoise, ME, demonstrated that the embayed nature of the Wells shoreline is a product of the regional bedrock structure intersecting the shoreline at an oblique angle creating bedrock headlands. They also speculated that the intervening arcuate beaches were formed from sediment derived from the erosion of glacial deposits. Hussey (1970) recognized that glacial forms were likely the anchoring points from which the present barrier spits now extend. These glacial forms may have also contributed some sand to the barriers of the region but the major source was probably from inland deposits.

Nelson (1979) believes that most of the sand comprising the Wells barriers came from the erosion of sandy

Presumpscot sediments and glacial outwash deposits in the Sanford region. These sands were transported to the coast via the Kennebunk River, Mousam River, Branch Brook, Merriland River and Webhannet River following deglaciation (Fig. 13). Nelson (1979) estimates that 1.6 x $10^8 m^3$ of sandy material was eroded from the upland region of these rivers. A determination of the actual volume will necessitate a more rigorous analysis of the topography, sedimentology, and paleo-drainage of the area. It is likely that the rivers debouched much of this sand during a period of lower sea level some distance offshore of the present coastline (Fig. 14). Thus, the barriers from Kennebunk south to Ogunquit consist of sand derived, in part, from reworked sands moved onshore during the Holocene transgression.

Radiocarbon dating of drowned stumps (Hussey, 1959) and marsh peats (Timson and Kale, 1976) in the Wells marsh indicates that barrier development in this region occurred approximately 3,000 yrs BP. It is probable that barriers existed prior to this time further offshore at lower sea levels, but these initial forms were unstable and highly transgressive. During this period of relatively rapid sea level rise (9,000 to 4,000 yrs BP; Fig. 14), the proto-barriers were likely thin, topographically low, discontinuous sand bodies that were migrating landward rapidly. In this setting it is unlikely that marsh formation

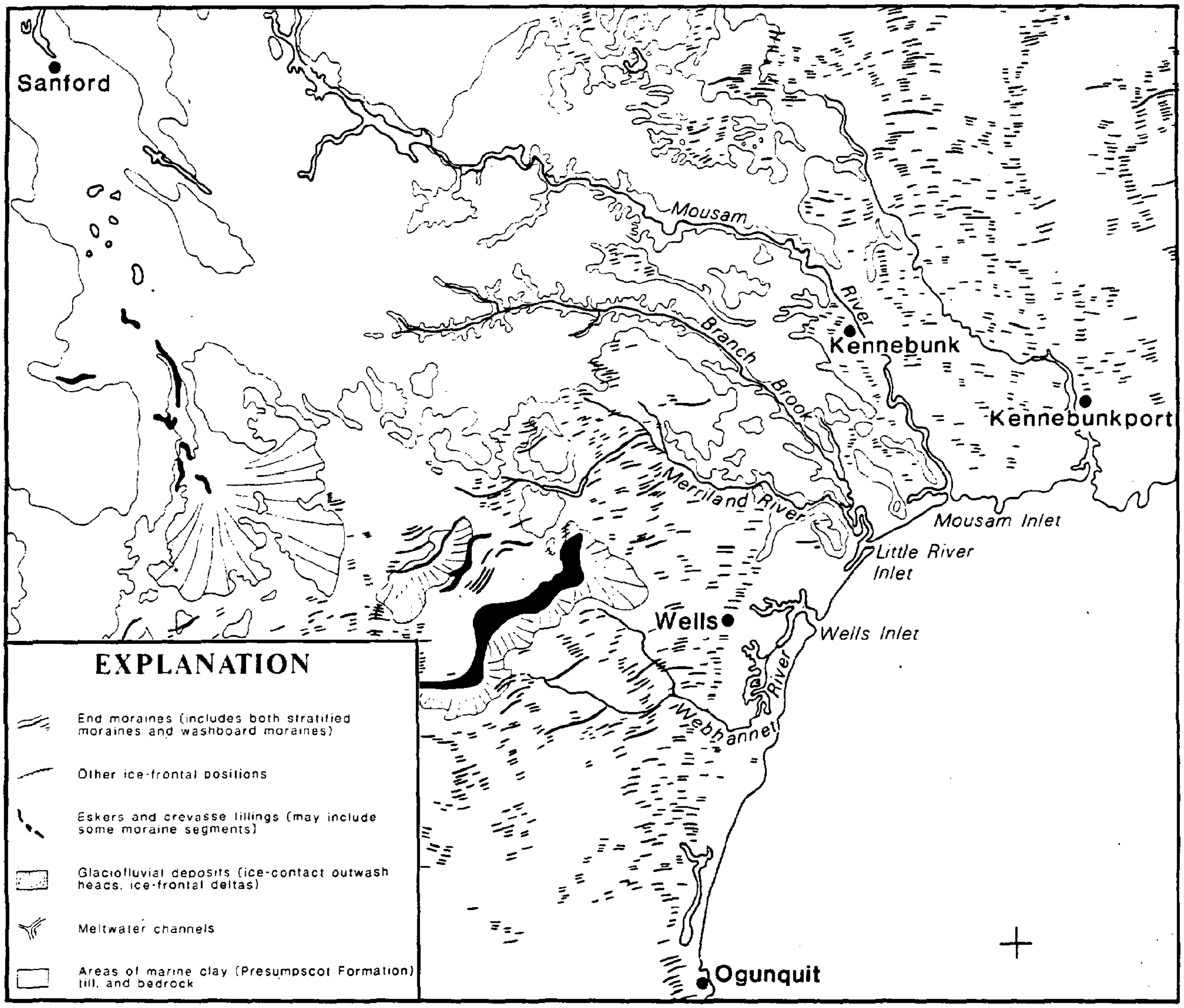


Figure 13. Glaciofluvial deposits in southeastern Maine (Modified from Smith, 1980).

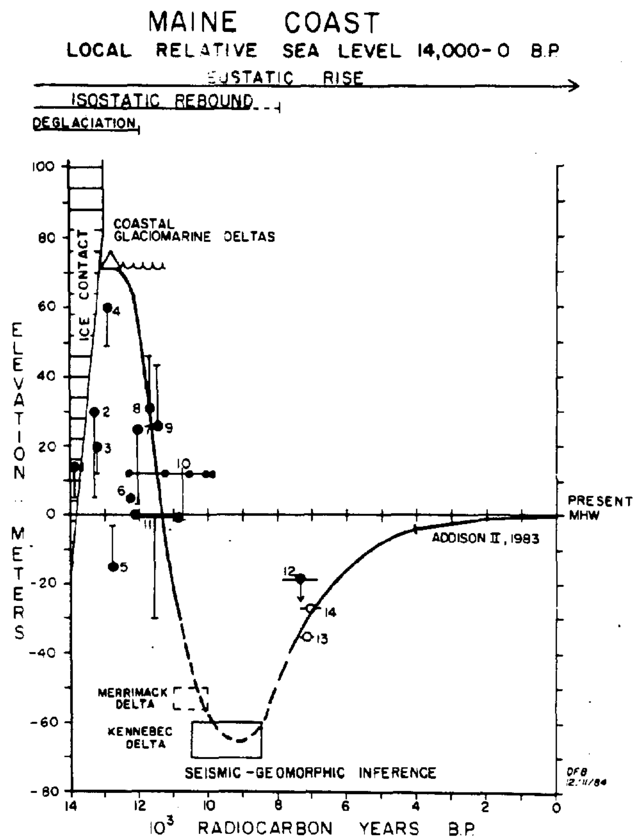


Figure 14. Sea level curve for the southern coast of Maine (from Belknap et al., 1988).

and peat production would have been substantial enough to be preserved in the transgressive coastal record. Not until the rate of sea level rise slowed were the transgressive barriers able to stabilize and for a short time become regressive. Once this state was reached, marshes accreted vertically with rising sea level (Kelley et al., 1988). As seen in cross sections of the Wells marsh, the peats in this area are generally thin, only 2 to 3 m thick, but in some cases can extend to 5 to 6 m (Fig. 15, McIntire and Morgan, 1963). Because of the similar settings and proximity, the marsh stratigraphy and peat thickness are likely the same for the Little River backbarrier.

As Hussey (1970) pointed out, barrier construction in the vicinity of Wells Beach, including Laudholm Beach and Crescent-Surf Beach, was tied closely to the presence of headlands and island areas. Although much of the sand comprising the present barrier system came from offshore, most of the barriers in this area probably developed as spits in a manner similar to that described for the Nova Scotian Northeast Coast by Boyd et al. (1988). The promontories from which these spits were initiated have largely disappeared, as they were originally glacial deposits that gradually were eroded. One of the pinning sites of the present barrier system still exists today along Drakes Island. The remnants of others are occasionally

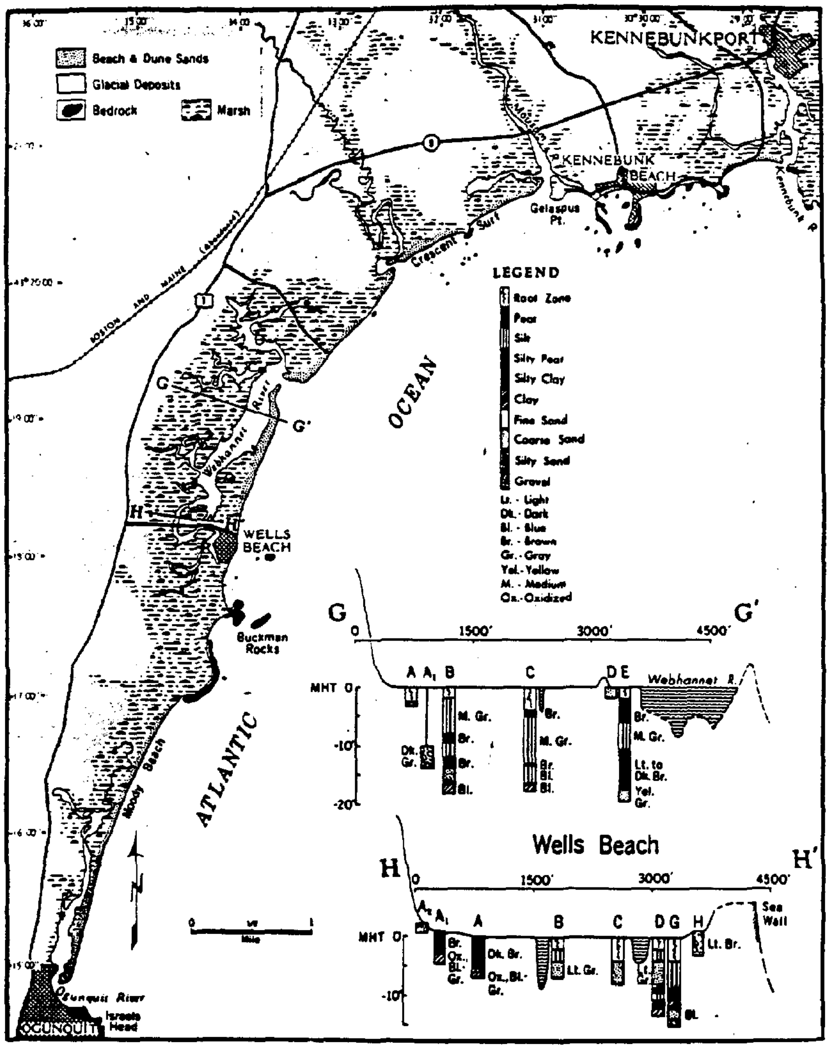


Figure 15. Stratigraphic section of the Wells back-barrier environment (from McIntire and Morgan, 1963).

exhumed after storms remove the overlying beach sediments.

## Inlet Development

The existence of Little River Inlet and other inlets along this stretch of shoreline is closely related to the presence of coastal river systems. However, the actual location of these inlets is not necessarily directly down slope of the river drainage. Often the river mouths (tidal inlets) are displaced along the coast by barrier spits. This is obvious at Ogunquit and Wells Inlets and less evident at Little River Inlet. Mousam River Inlet was once displaced to the northeast by a barrier spit, but was artificially moved to its present site southwest side of Great Hill in the mid-1800's (Nelson, 1979).

The oldest map of this region is a British Admiralty chart of the Wells area in the 1770's (Fig. 16, Fink et al., 1984). This chart, while not correct in every detail, does accurately depict the sites of tidal creeks and the location and general morphology of most major waterways. As seen in figure 16, Little River Inlet in the 1770's was in the same approximate position as it is today. Like the present inlet system, the inlet channel in 1770 took a sharp clockwise meander before meeting the ocean (Fig. 17).

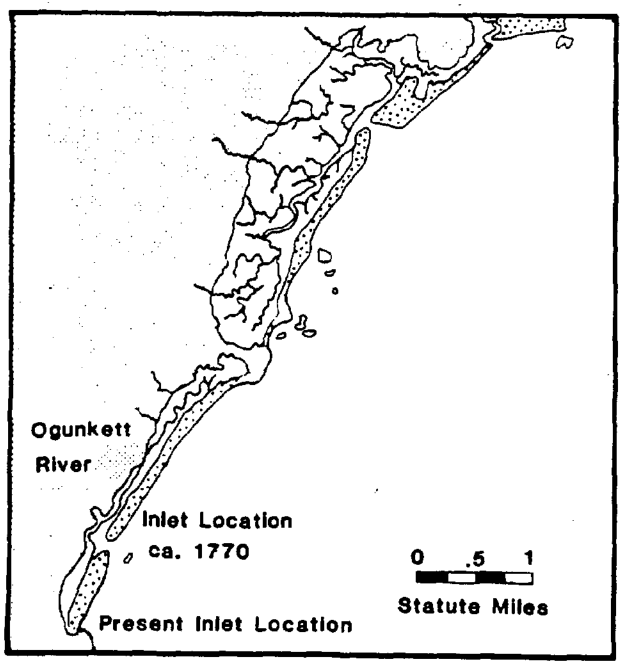


Figure 16. Redrawn map of a portion of a 1770's vintage British chart of the Wells region (from Fink et al., 1984).

Figure 17. 1988 oblique aerial photograph of Little River Inlet showing the low tide sand bodies.

# INLET MORPHOLOGY

## Historical Changes

Aerial photographs dating back to 1940 indicate that the entrance channel at Little River Inlet has undergone a cyclic pattern of change over at least the last 46 years (Fig. 18). Between 1940 and 1953 (Fig. 18, A and B), the inlet channel breached Crescent Surf Beach spit to the north, and southern Laudholm Beach spit accreted northeastward. Most of the sand isolated by the breaching event along Crescent Surf Beach became flood-tidal delta deposits. Within the next 20 years (Fig. 18, C), Crescent Surf Beach spit began accreting in a southerly direction and the end of Laudholm Beach spit migrated landward attaching to the flood-tidal delta region. By 1974 (Fig. 18, D), Crescent Surf Beach spit had prograded to the position that was present in 1940. At the same time, the southwestern deflection of the inlet severed the curved end of Laudholm Beach spit, leaving the landward portion of this sand as a flood-tidal delta region. The orientation of the inlet has not changed significantly between 1986 and 1988.

Accretion on both the north and south spits occurs as a result of the seasonal variation in longshore sediment transport direction characterizing that area, and breaching of the spits occurs during large storm events when the inlet

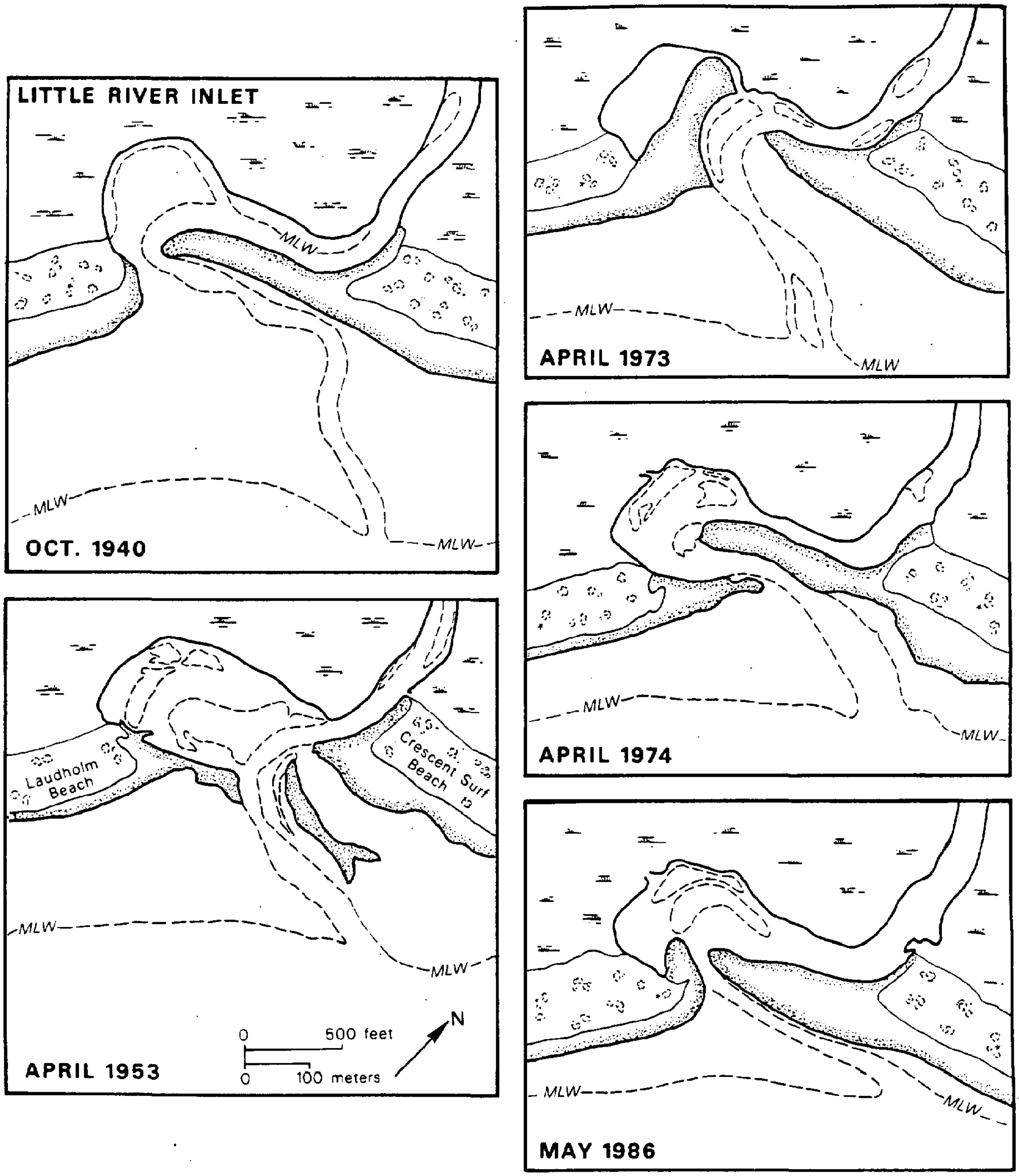


Figure 18. Morphological changes at the inlet from 1940 to 1986 as determined from vertical aerial photographs.

channel establishes a more efficient pathway for water exchange between the ocean and backbarrier. If this spit accretion/breaching cycle continues, the present elongated Crescent Surf Beach spit should be breached in the next ten years, shifting the location of the inlet throat to a more northerly position. However, the southwestern end of Crescent Surf Beach spit is relatively wide and has a well-established dune system making spit breaching difficult.

Recent Inlet Changes

Recent morphological changes at the inlet can be discerned from oblique aerial photographs taken of the inlet in March 1986 and 2.6 years later in October 1988 (Fig. 19). During this period several changes can be noted:

1. The spit system on the northeast side of the inlet at the southern end of Crescent Surf Beach has accreted slightly to the southwest.
2. Flood-tidal delta sands have been pushed further southwest into the backbarrier and the entire deposit has been displaced to the southwest.
3. The northern spit end of Laudholm Beach experienced accretion and more sand was added to the landward, recurved portion of the spit.
4. Dune development along the southwestern end of Crescent Surf Beach has vertically built up that portion of the spit.

Figure 19. Oblique aerial photographs of Little River Inlet, A. March, 1986 and B. October, 1988.

5. The outer part of the inlet channel changed its course to a straighter, more direct route to the ocean. This was accomplished either by a gradual migration process or was a result of ebb-tidal delta breaching.

## CHANNEL CROSS SECTIONS

The present channel morphology at Little River Inlet is illustrated in detail in Figures 20-27. At the seaward end of the inlet, the channel cross section is essentially symmetrical, with maximum depths between 0.5 and 1.5 m below MSL (Figs. 21 and 22). Further landward, the channel thalweg (Fig. 20) becomes asymmetric in cross section, with greater depths occuring along Laudholm Beach spit. This morphology is due to the ebb currents being directed at Laudholm Beach spit and is a common characteristic of a meandering channel system.

A series of eight channel surveys taken over a ten-month period at three locations at the inlet entrance channel indicates that the position of the channel is currently very stable (Figs. 23-25). Although these surveys indicate that the channel depth has varied through this time, the exact amount, as well as trends, cannot be established with the

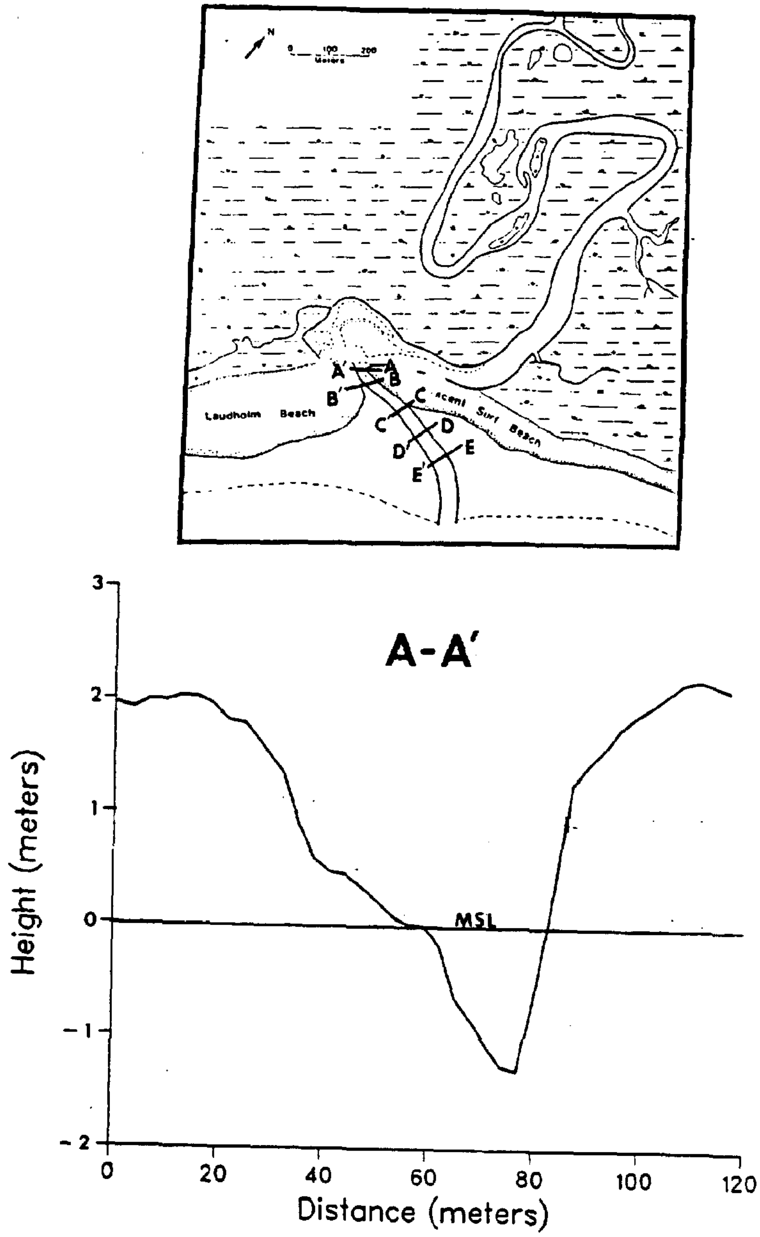


Figure 20. Bathymetric profile location map and profile of the inlet throat at Little River.

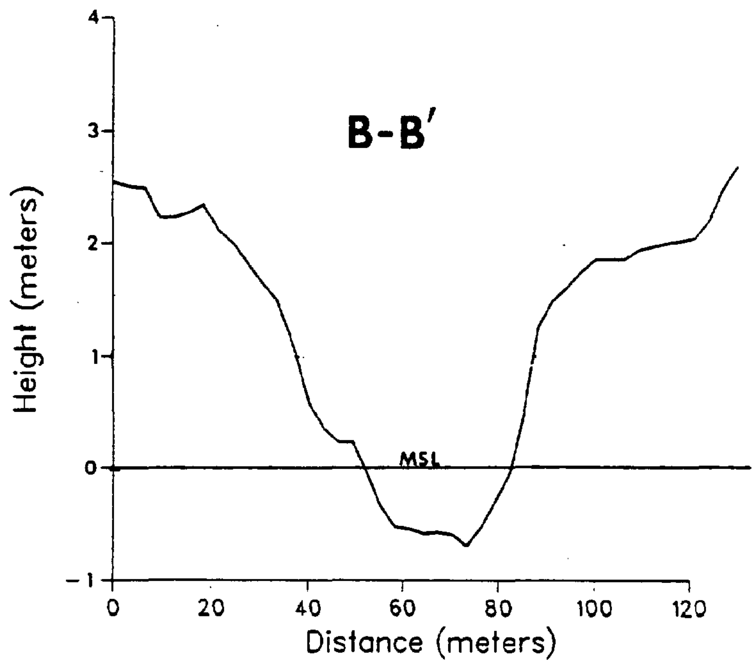


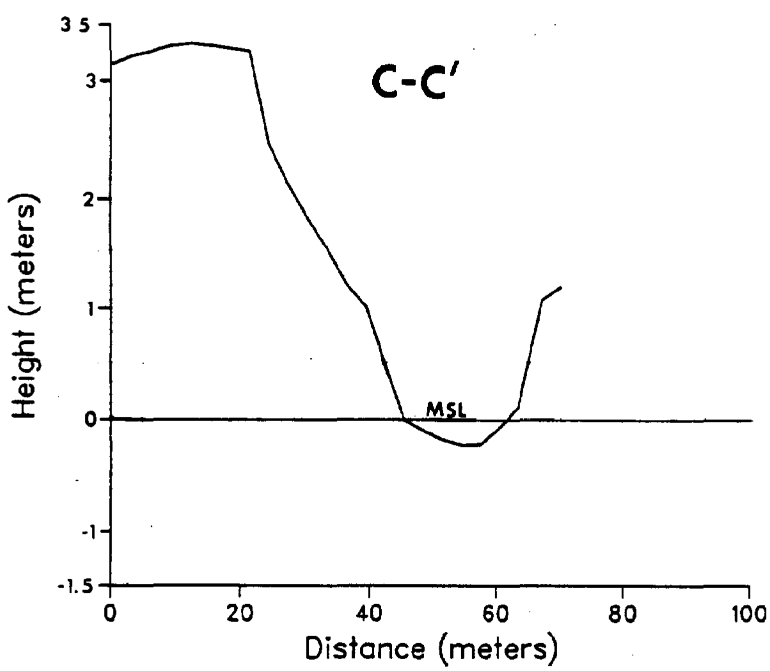


Figure 21. Bathymetric profiles at the Little River Inlet entrance channel.

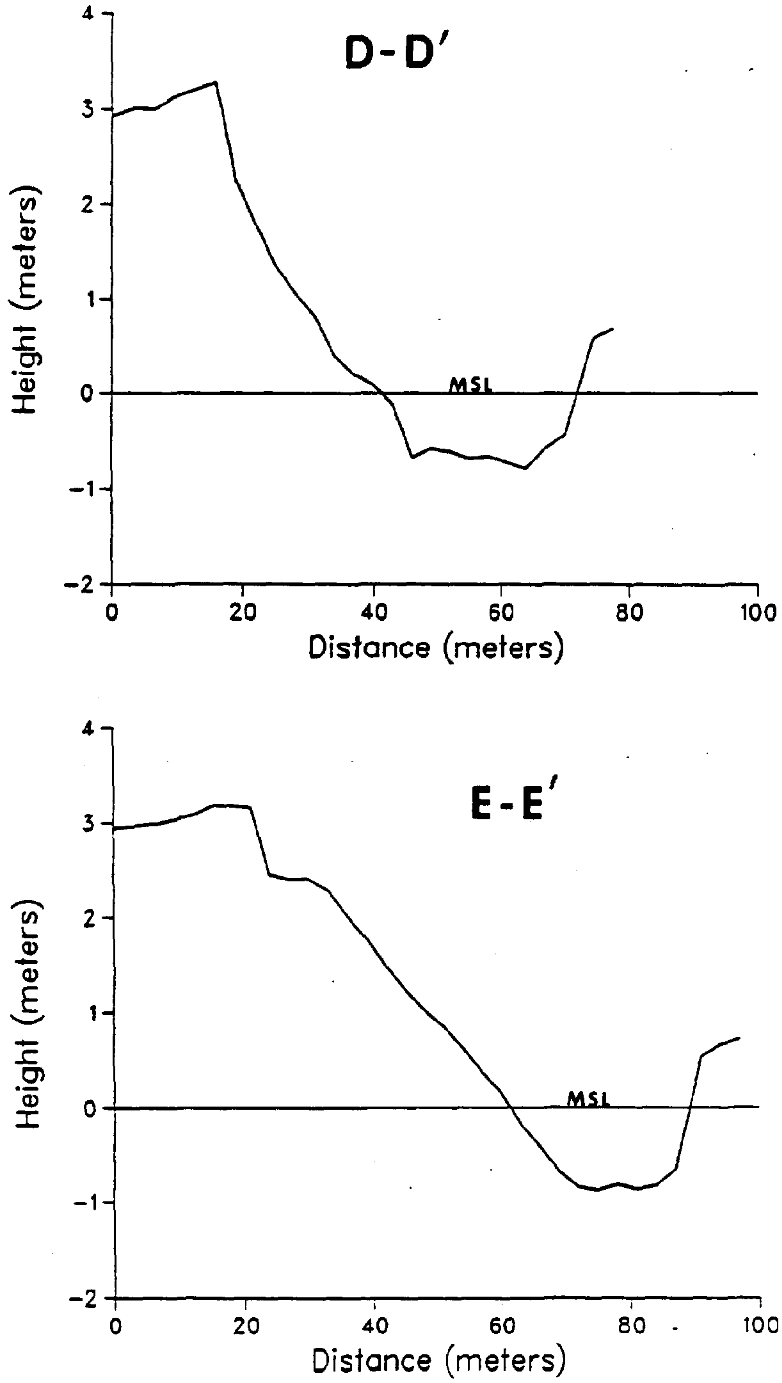


Figure 22. Bathymetric profiles at the Little River Inlet entrance channel.

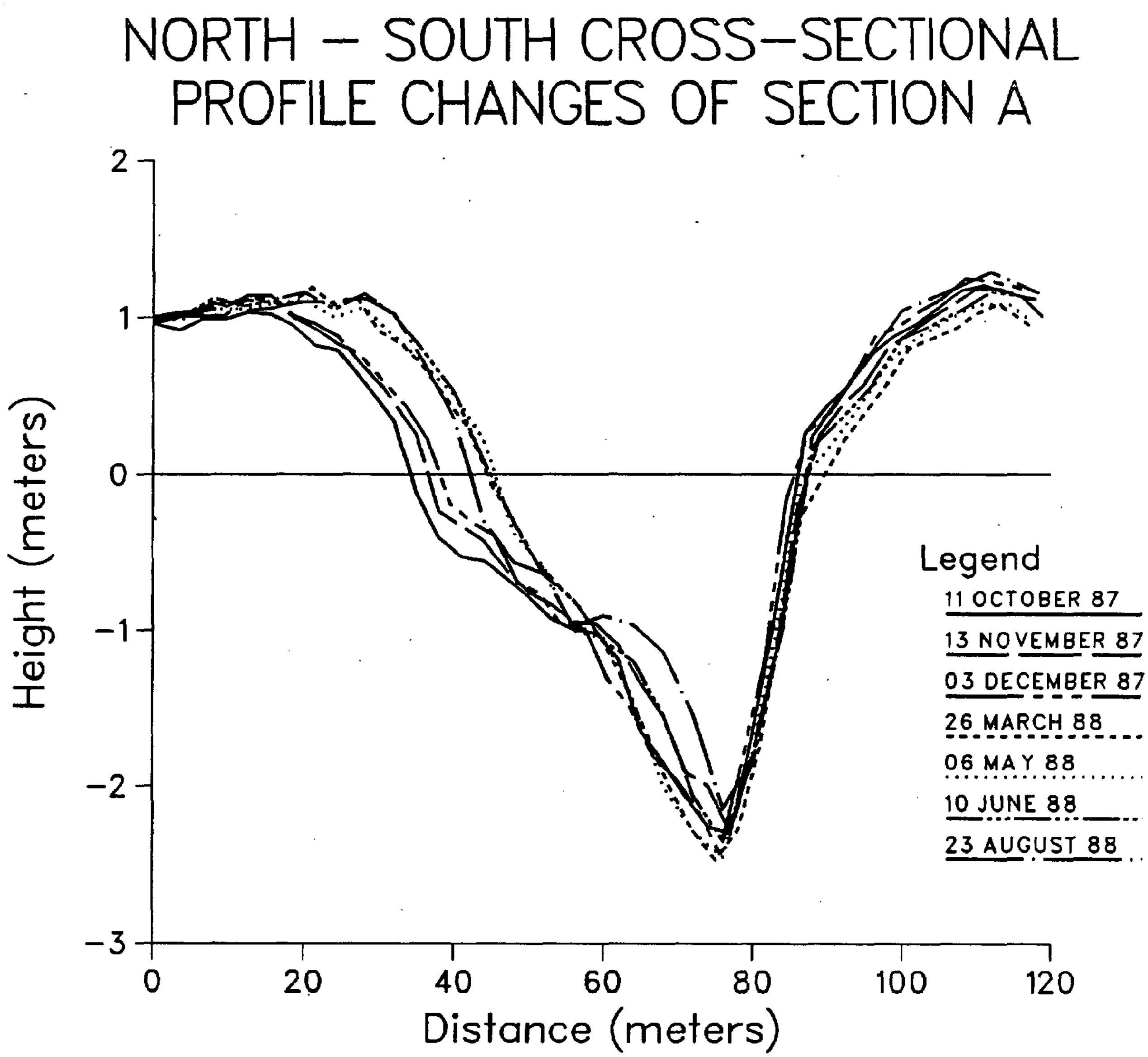


Figure 23. Sequential channel surveys taken at the Little River Inlet throat. Notice the small degree of channel displacement over this period.

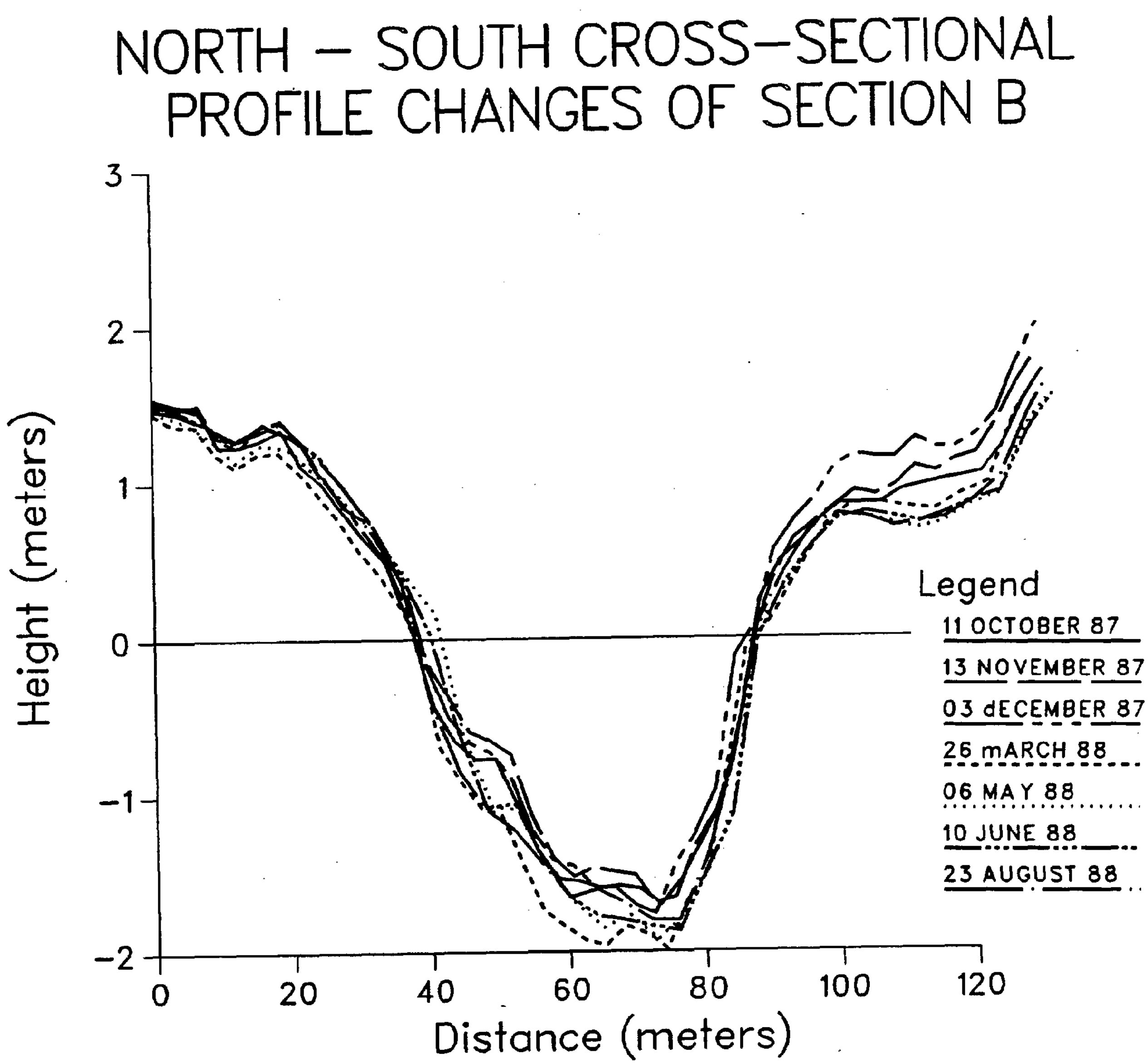


Figure 24. Sequential channel surveys taken at the Little River Inlet entrance channel.

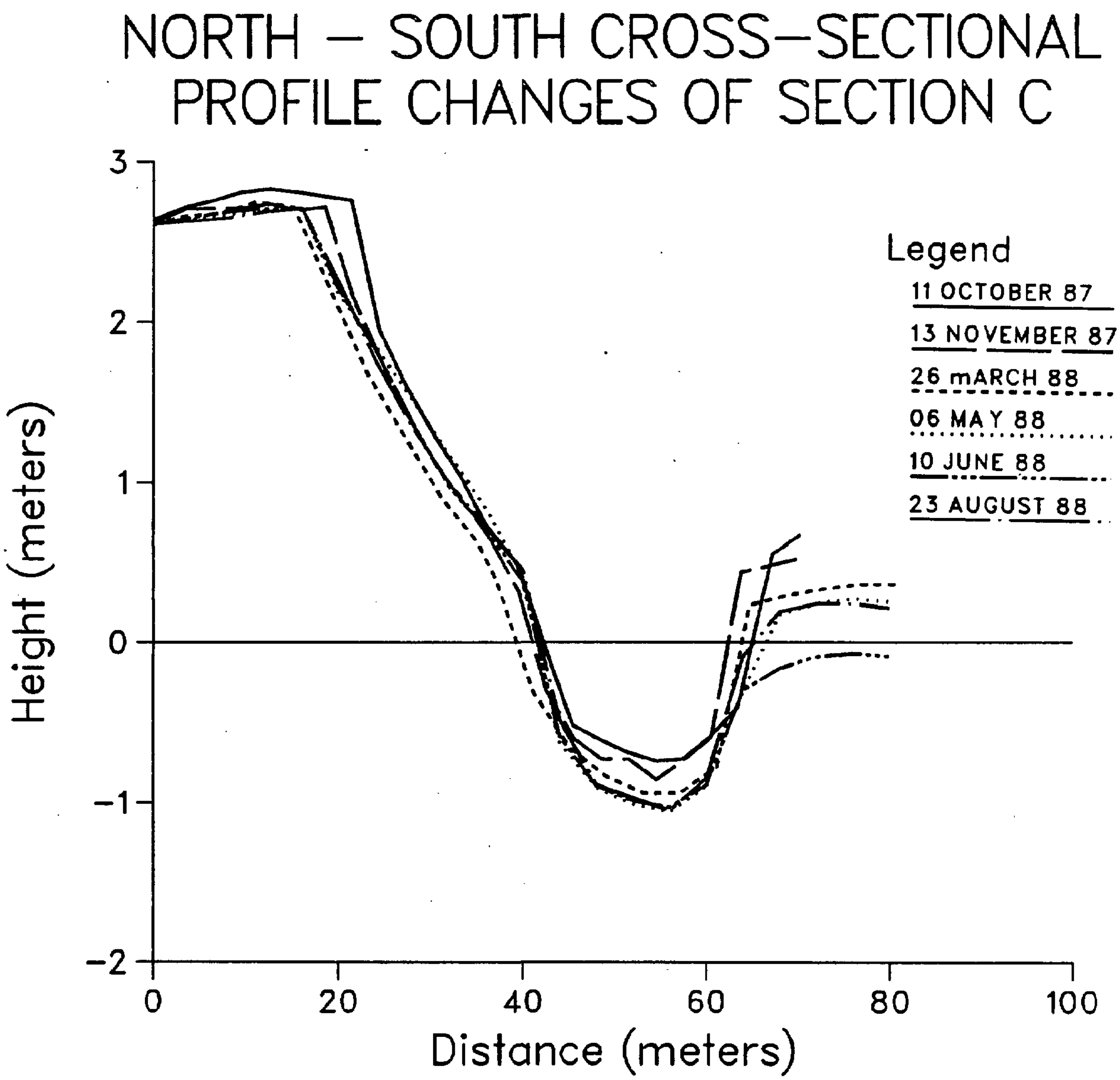


Figure 25. Sequential channel surveys taken at the Little River Inlet entrance channel.

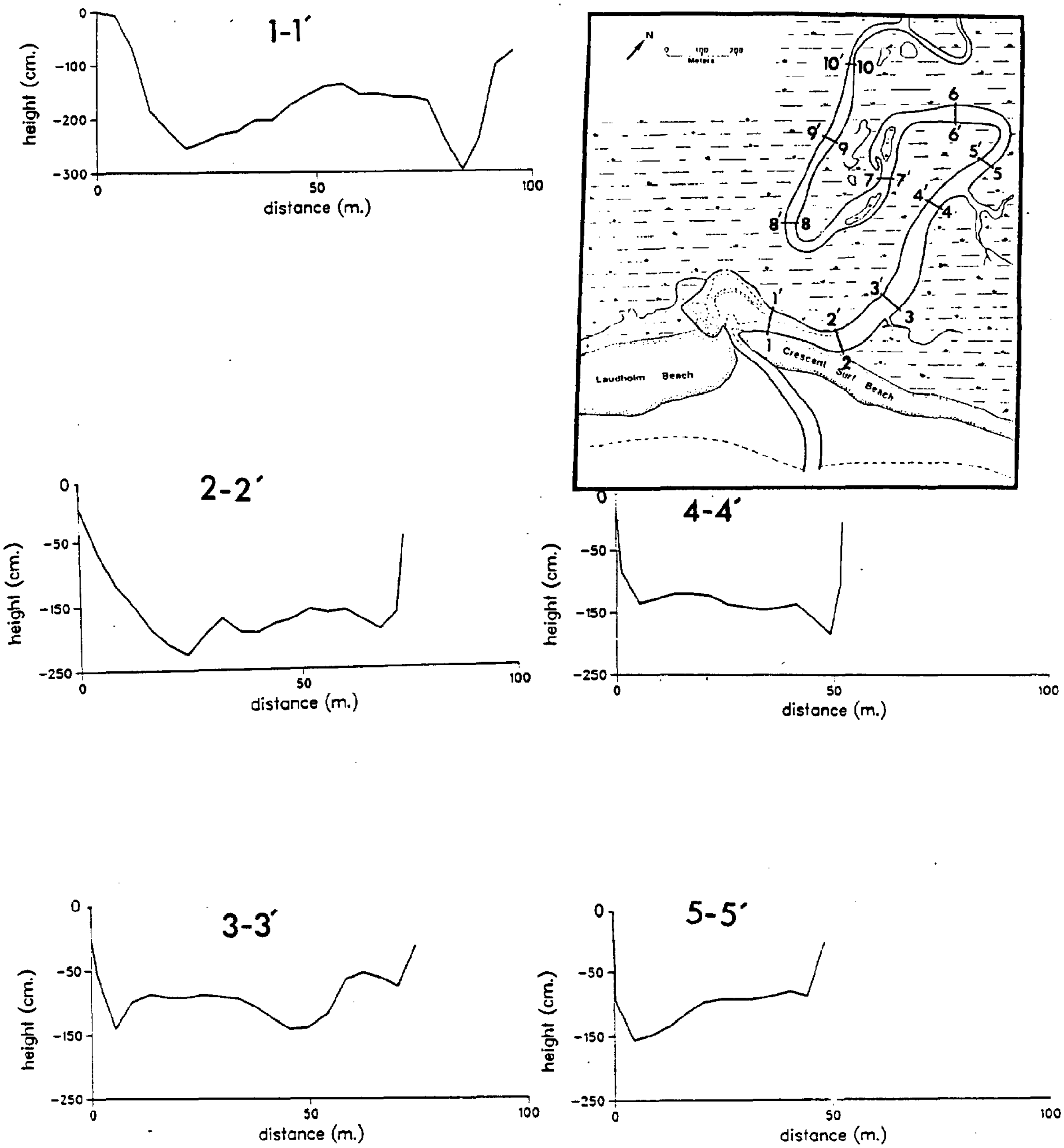


Figure 26. Bathymetric profiles of the backbarrier region in 1988.

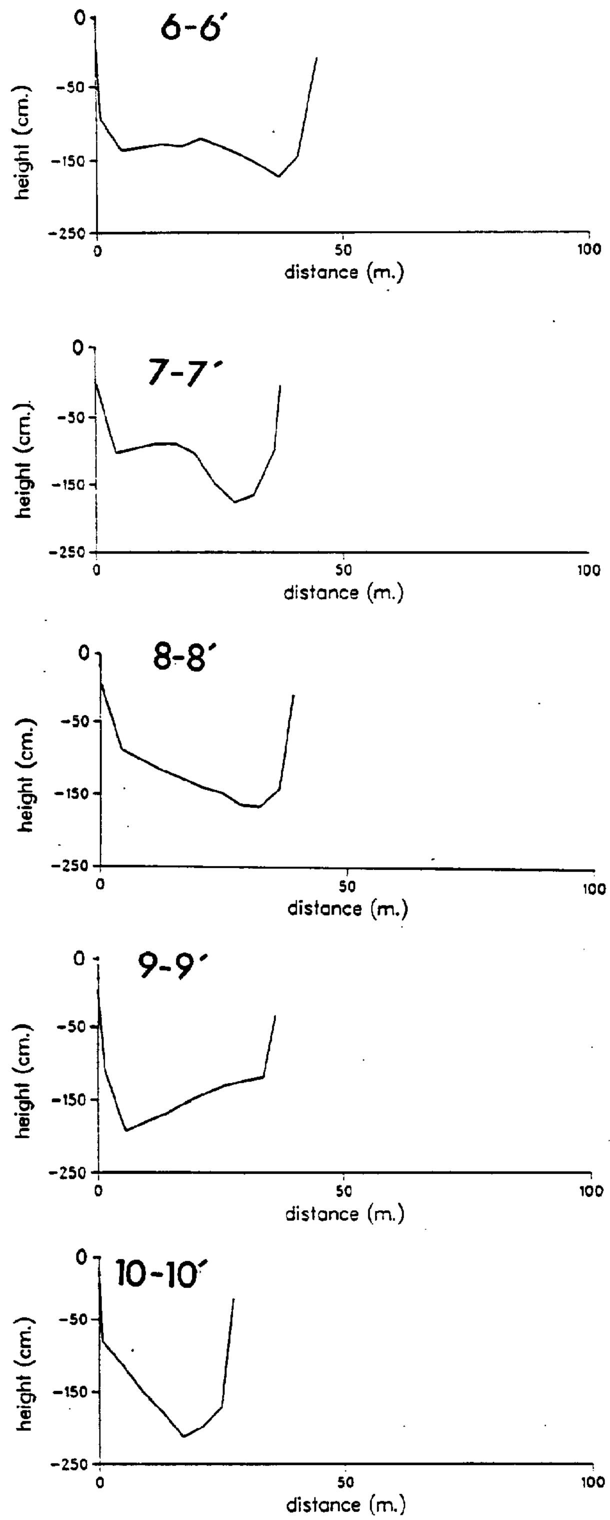


Figure 27. Bathymetric profiles of the backbarrier region in 1988.

existing database.

Moving to the backbarrier region, Sections 1-1' and 2-2' (Fig. 26) exhibit the subtidal continuation of the flood-tidal delta with greatest depths occurring on the sides of the channel. Further landward, the channel gradually develops a meandering, asymmetric character, typical of a river meander system (Sections 3-3' to 10-10', Figs. 26 and 27).

## SEDIMENT CHARACTERISTICS AND TRENDS

Like Wells Inlet, Little River Inlet is composed predominantly of sandsized material with cobble material and/or mud occuring as minor constituents in other areas (Fig. 28). Gravel is found along the channel thalweg in the intertidal zone where there are strong tidal currents. Gravel also occurs on the sides of the channel, on the northern tip of Laudholm Beach spit, and at a few sites in the backbarrier channel. Like Wells Inlet, these occurrences probably represent lag deposits from the reworking of till or storm deposits.

Mud occurs throughout most of the upper backbarrier region as a minor constituent (<5%), except at one location where the mud content is approximately 60% (Fig. 28). Mud

Little River Sediment Samples

1. Sand (-0.66), Cobbles
2. Sand (-1.54), Cobbles
3. Sand (0.29)
4. Sand (-0.75), Cobbles
5. Cobbles
6. Sand (-0.41)
7. Sand (0.84), Cobbles
8. Sand (-0.28), Cobbles
9. Sand (2.21)
10. Sand (-2.10), Cobbles
11. Sand (0.41)
12. Sand (0.87)
13. Sand (1.43)
14. Sand (2.05), Cobbles
15. Sand (1.30)
16. Sand (2.33)
17. Sand (1.42)
18. Sand (2.47), Mud (0.57%)
19. Sand (2.50)
20. Sand (1.96)
21. Sand (1.40)
22. Sand (1.03)
23. Sand (1.15), Cobbles
24. Sand (1.34)
25. Sand (2.06)
26. Sand (1.98), Mud (2.06%)
27. Sand (1.75)
28. Sand (1.56), Mud (0.24%)
29. Sand (1.50)
30. Sand (2.04), Mud (0.55%)
31. Sand (2.00), Mud (4.92%)
32. Sand (1.69), Cobbles, and Mud (59.26%)
33. Sand (1.51), Mud (2.52%)
34. Sand (1.73), Mud (4.22%)
35. Sand (0.93), Cobbles, and Mud (9.70%)

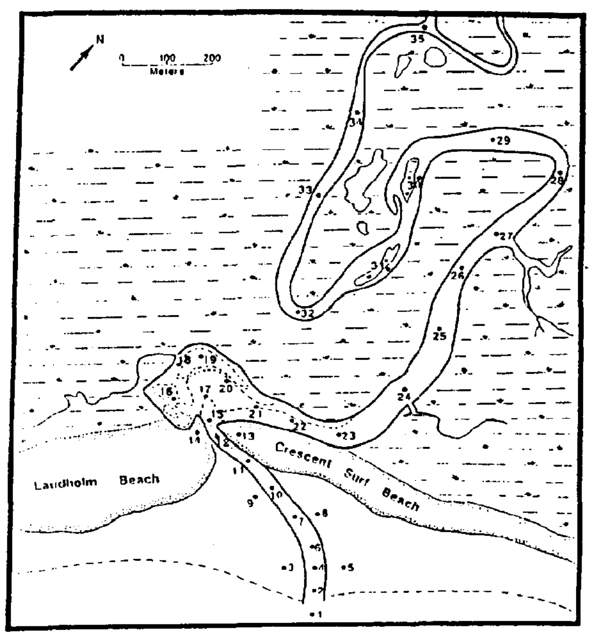


Figure 28. Location and description of bottom samples collected in the inlet channel. Mean grain sizes in phi units are given for the sand fraction.

was also found on the back edge of the flood-tidal delta. The source of the mud may be from the Merriland River or Branch Brook during large floods or it may come from the ocean. There are several sites in the offshore region where till is being excavated by wave action, releasing fine-grained material in the water column. In either case, mud may be deposited in the backbarrier in quiet water areas.

Mean grain size and grain sorting maps have been produced for the sand fraction of each sample at Little River Inlet (Figs. 29 and 30). The two maps tend to correlate fairly well with the tidal current patterns existing throughout the inlet. Sands generally become finer-grained and better sorted in a landward direction, where tidal currents progressively decrease. The finest, most well-sorted sand occurs along the periphery of the flood-tidal delta where tidal currents are relatively weak (<10 cm/sec).

## TIDAL HYDRAULICS

### Tidal Currents

Current velocities were measured at five locations along the inlet channel during spring, mean and neap tidal conditions (Fig. 31). The tide curves and velocity time-series of these hydrographies are given in Figures 32-34. The pertinent data from these surveys are summarized in

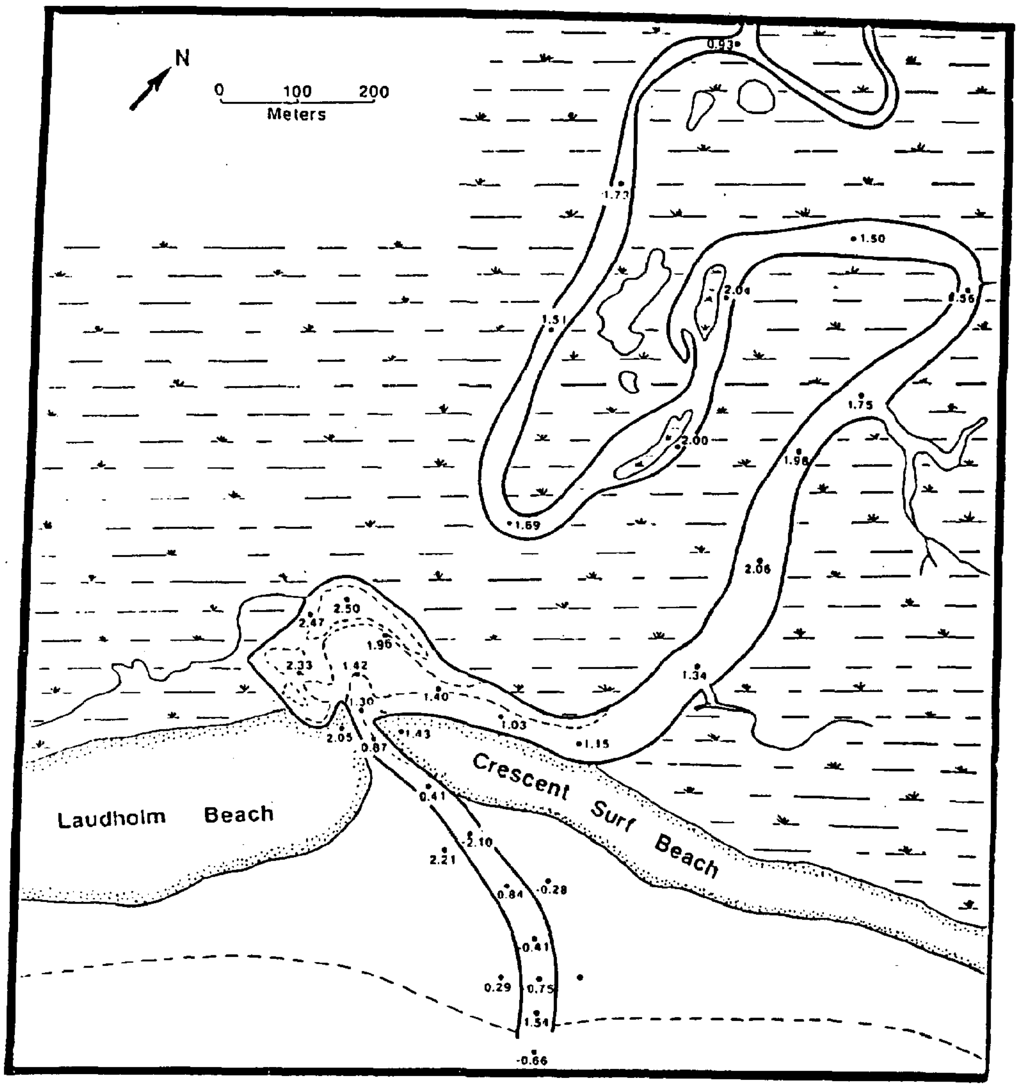


Figure 29. Mean grain size distribution at Little River Inlet.

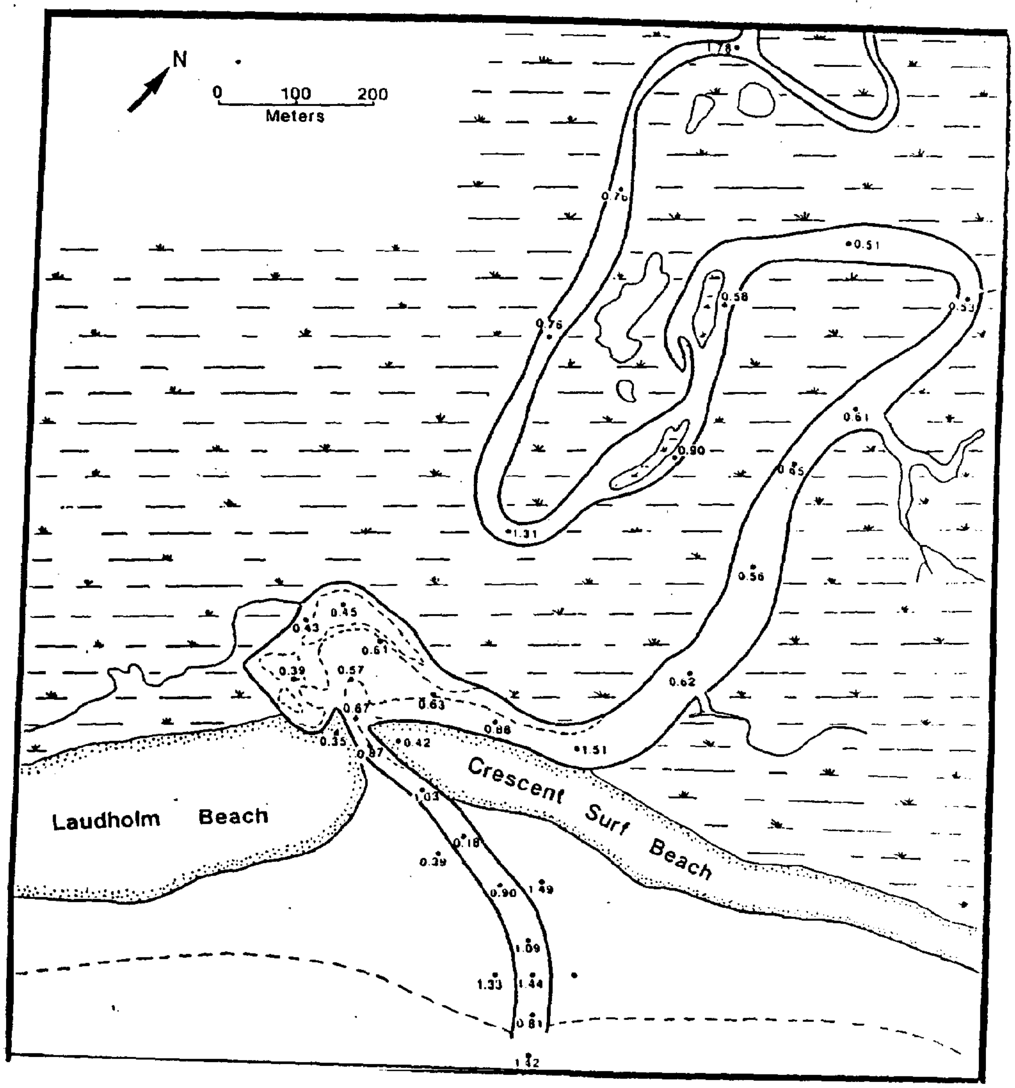


Figure 30. Grain sorting distribution at Little River Inlet.

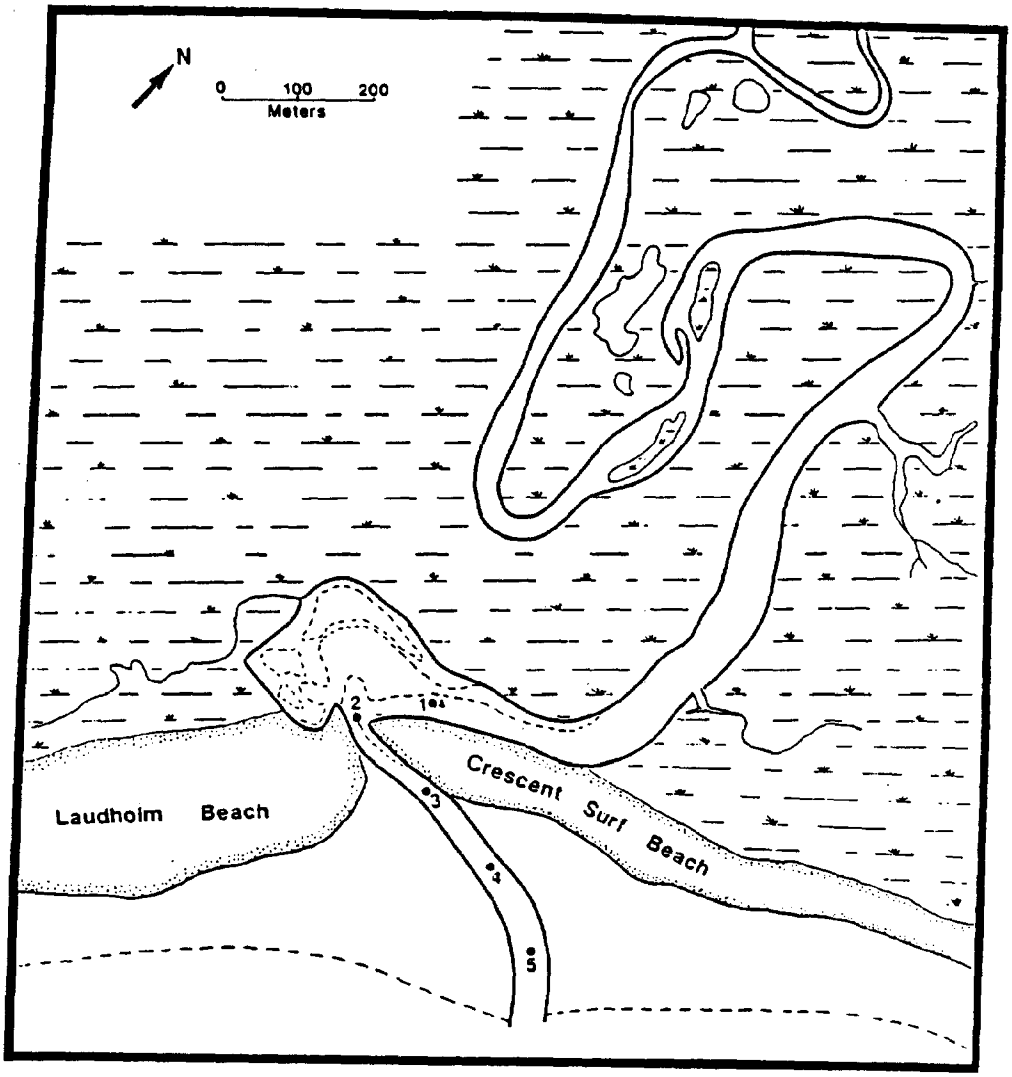


Figure 31. Location of hydrography stations at Little River Inlet.

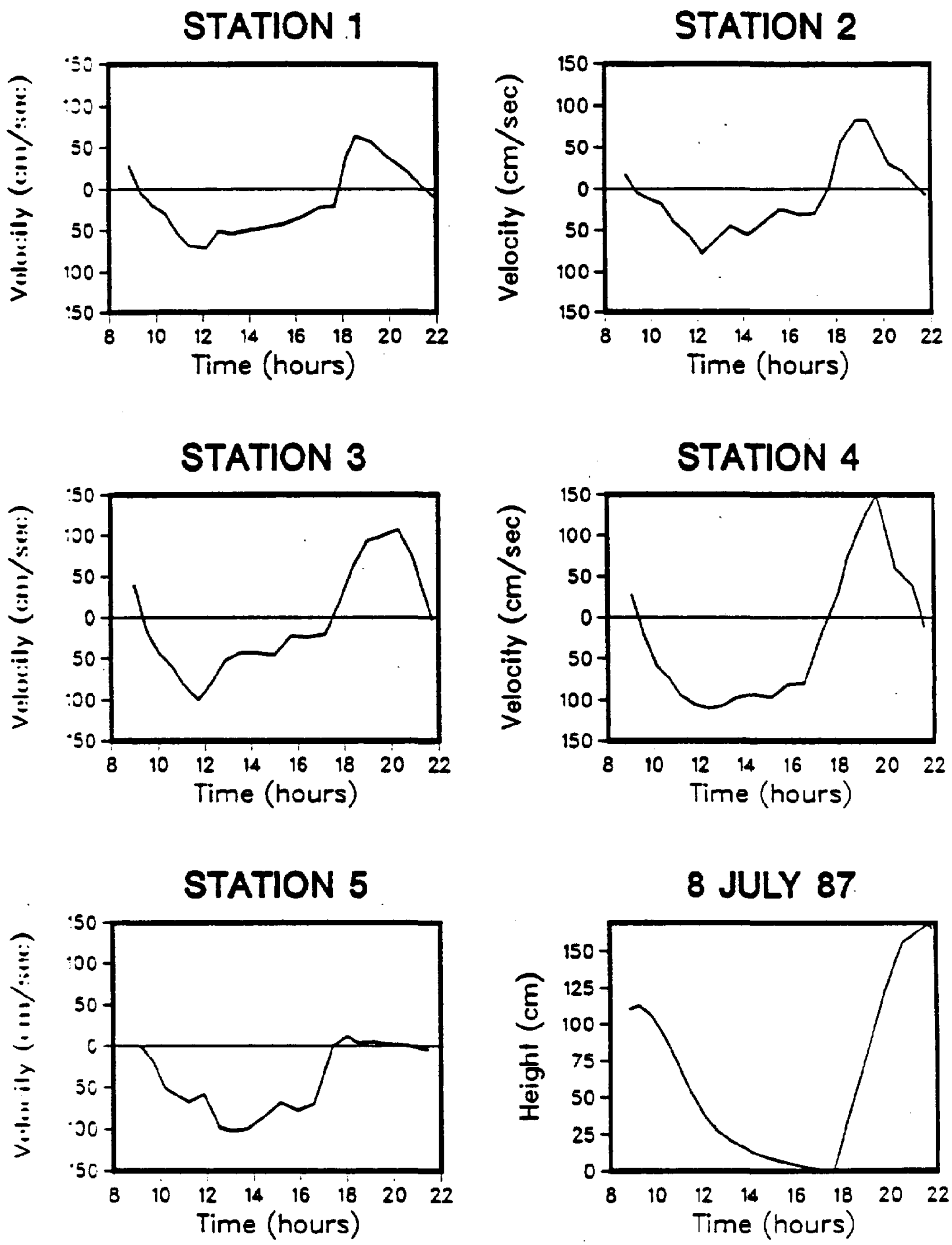


Figure 32. Velocity-time series and tide curve for stations 1-5 on 8 July 1987.

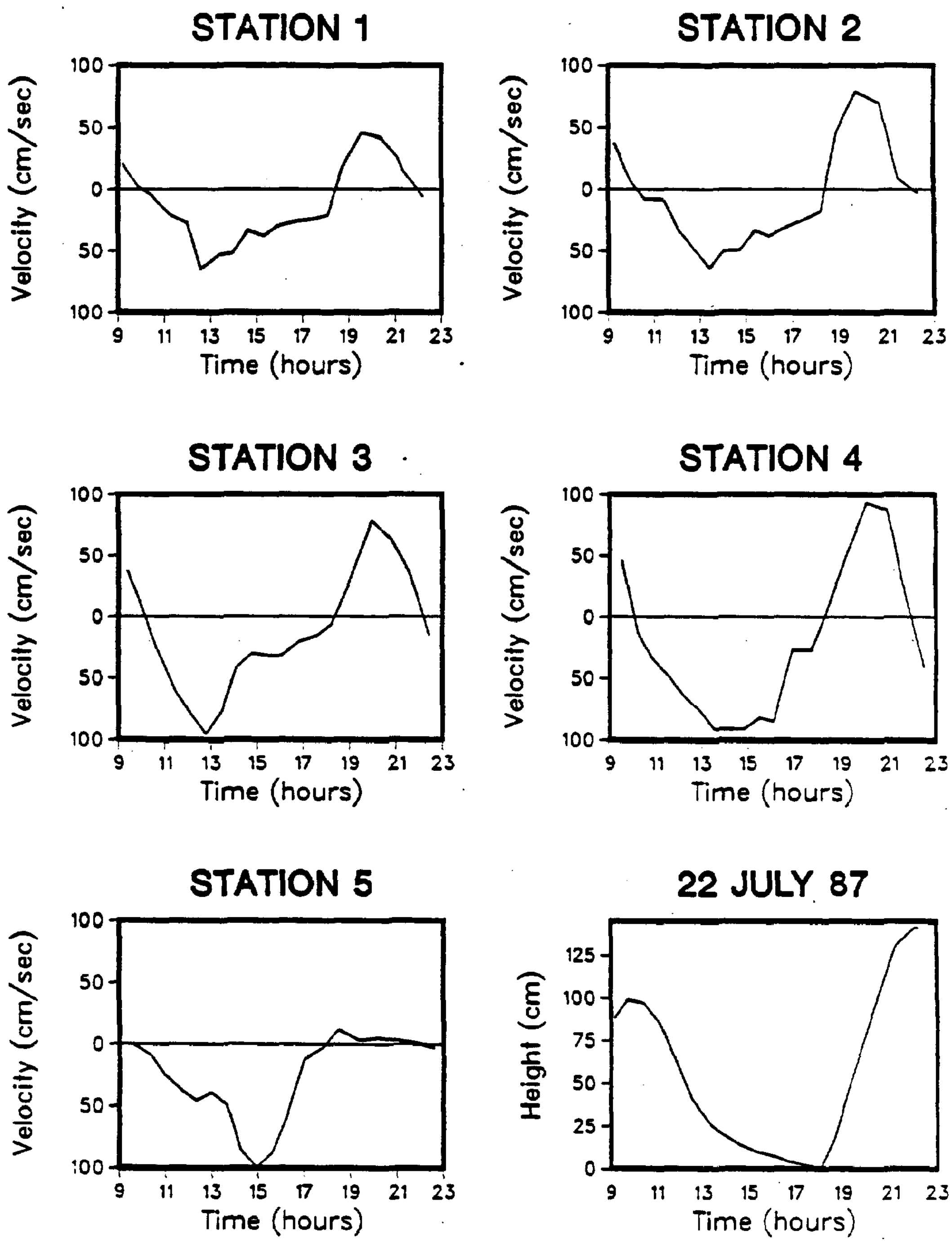


Figure 33. Velocity-time series and tide curve for stations 1-5 on 22 July 1987.

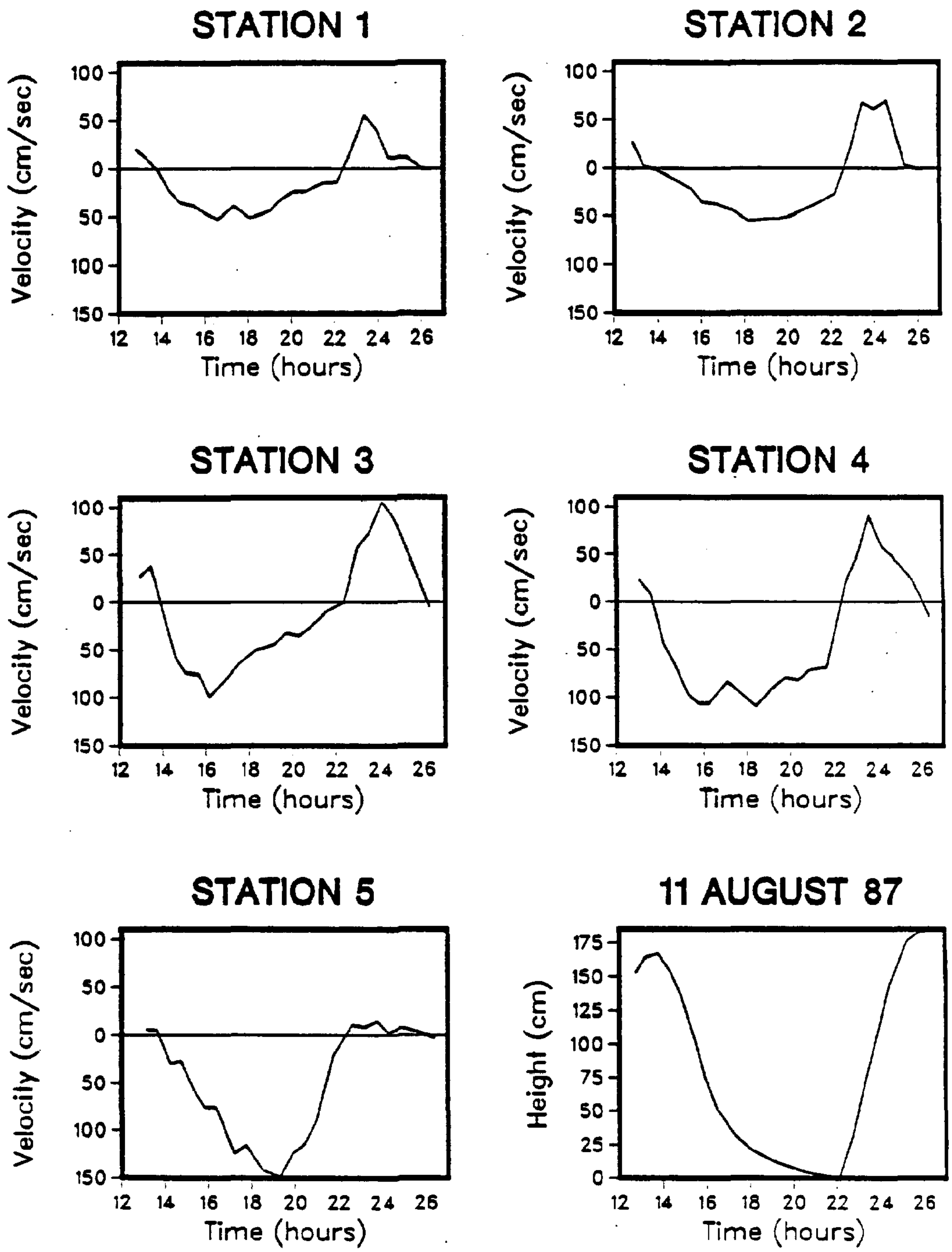


Figure 34. Velocity-time series and tide curve for stations 1-5 on 11 August 1987.

TABLE 1.

Summary of Hydrographic Data for Inlet Throat

| DATE | MAX. VEL. (cm/sec) | | MEAN VEL. (cm/sec) | | TIDAL DURATION (hr:min) | | TIDAL RANGE (cm) | |
|---|---|---|---|---|---|---|---|---|
| | Fld | Ebb | Fld | Ebb | Fld | Ebb | Fld | Ebb |
| 08Ju87 | 83 | 79 | 45 | 38 | 3:50 | 8:20 | 169 | 113 |
| 22Ju87 | 79 | 64 | 46 | 33 | 3:54 | 8:05 | 143 | 98 |
| 11Au87 | 70 | 55 | 40 | 35 | 3:15 | 9:00 | 184 | 167 |

TABLE 2.

Summary of Maximum Currents for Channel Thalweg Stations

| DATE | STA. 1 (cm/sec) | | STA. 3 (cm/sec) | | STA. 4 (cm/sec) | | STA. 5 (cm/sec) | | TIDAL RANGE (cm/sec) | |
|---|---|---|---|---|---|---|---|---|---|---|
| | Fld | Ebb | Fld | Ebb | Fld | Ebb | Fld | Ebb | Fld | Ebb |
| 08Ju87 | 64 | 72 | 107 | 100 | 150 | 110 | 12 | 102 | 169 | 113 |
| 22Ju87 | 46 | 65 | 79 | 96 | 94 | 91 | 12 | 100 | 143 | 98 |
| 11Au87 | 56 | 53 | 106 | 99 | 91 | 106 | 15 | 149 | 184 | 167 |

Tables 1 and 2. As tidal forcing is the primary control of current magnitude, mean and maximum velocities have been plotted against tidal range for the inlet throat station (Figs. 35 and 36). While there is insufficient data to do regression analysis, it is clear from the plots that the inlet throat is dominated by flood tidal currents. Maximum flood currents ranged from 70 to 83 cm/sec, while maximum ebb currents varied from 55 to 79 cm/sec. Similarly, mean flood velocities (40-45 cm/sec) exceeded mean ebb velocities (33-38 cm/sec) by an average of 7 cm/sec (Table 1).

As seen in Table 2, the stronger flood than ebb currents at Little River Inlet are a result of the ebb duration averaging more than 4 hours longer than the flood duration. If the freshwater discharge is neglected and it is assumed that the flood tidal prism equals the ebb prism, then because there is more time to empty the backbarrier than to fill it, the flood currents must move more swiftly than the ebb currents.

Stations 1 through 5 are located in the inlet channel both seaward and landward of the throat (Fig. 31). While Stations 3 and 4 appear to possess slightly stronger flood currents, Stations 1 and 5 are clearly ebb-dominated (Table 2; Figs. 32-34). Like Wells Inlet the ebb dominance of the backbarrier station (Station 1; Fig. 31) at Little River Inlet is explained by segregation of flow such that

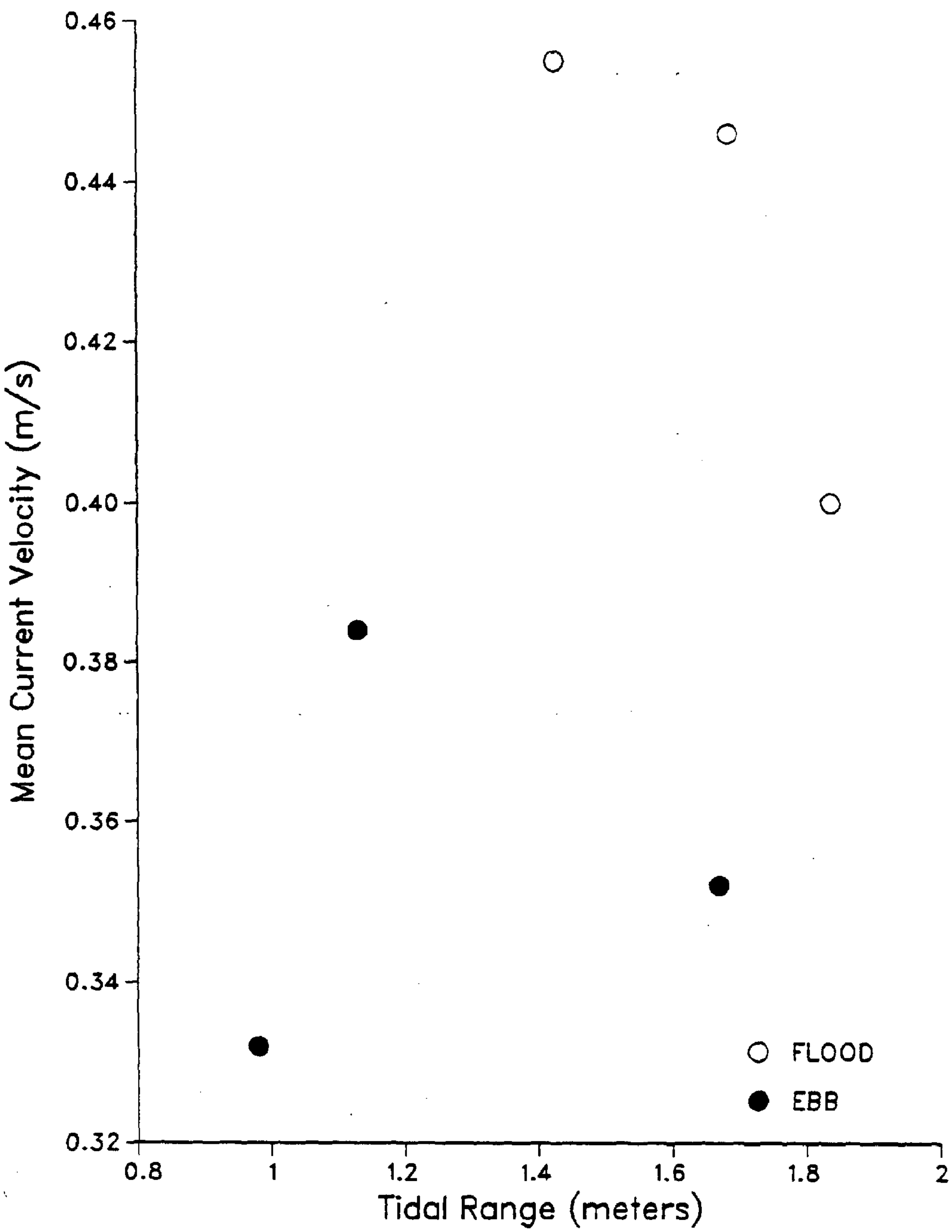


Figure 35. Plot of mean current velocity versus tidal range at the inlet throat for flood and ebb cycles. Note the dominance of the flood tidal currents.

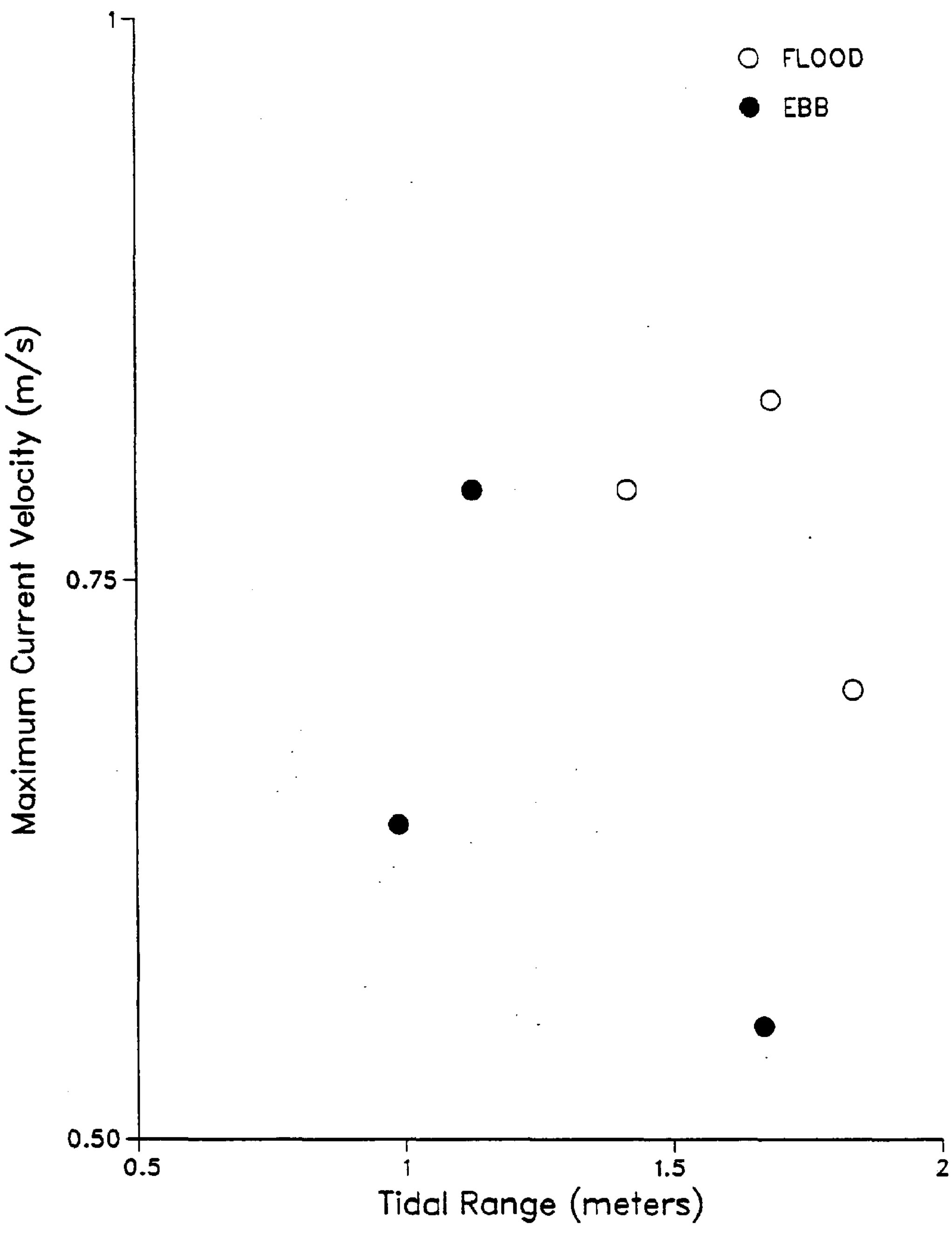


Figure 36. Plot of maximum current velocity versus tidal range at the inlet throat for flood and ebb cycles. Note the dominance of the flood tidal currents.

the maximum ebb currents are confined to the channel thalweg while the flood currents are spread over the entire channel cross section. Station 5 is ebb dominated because it is positioned relatively close to the inlet-channel/ocean-low-tide interface and the rising tide quickly overflows the channel banks. The large increase in cross sectional area greatly diminishes the flooding currents almost immediately after the flood tide begins.

## Discussion

Little River Inlet is dominated by shorter flood than ebb durations resulting in a flood-dominated hydraulic character. Similar findings have been documented by Lincoln and FitzGerald (1988) at several small tidal inlets in Maine. They attribute the shorter flood durations, in part, to the formation of overtides (M4, M6, M8 tidal constituents). More important, Lincoln and FitzGerald (1988) explain the flood dominance of these inlets as a result of the shallow channel morphology. This condition causes a truncation of the tidal wave as it propagates through the inlets, resulting in an extended period of low slack water and, hence, a short flood duration. This condition occurs at Little River Inlet and is believed to be the primary control of tide asymmetry.

A sill, comprised chiefly of cobbles and some boulders, exists 50 m seaward of the throat section at Little River Inlet (Fig. 37). The sill is believed to be a coarse gravel lag that was left behind when the original glacial deposit was eroded away. As the tide falls during the ebb cycle, the sill gradually retards the flow of water out of the inlet by effectively reducing the hydraulic slope in the inlet channel. The presence of the sill diminishes the potential strength of the flood and ebb currents, as well as the tidal range in the backbarrier.

The elevation of the sill is 1.21 m above the height of ocean mean low water (Fig. 37). Consequently, flood currents do not occur at the inlet until the ocean tide is well into the flood cycle. This leads to a long ebb duration (8 to 9 hrs) characterized by an extended period (2 to 3 hrs) of relatively weak ebb currents (vel. < 35 cm/sec). Because the height of the sill is only 10 cm below mean sea level, when flood waters overtop the sill the ocean tide is in its period of most rapid rise. Thus, low slack water at the inlet lasts only momentarily and then, the currents are reversed and the water level rises quickly at the inlet. This condition, which results in maximum flood velocities occurring very early in the flood cycle (of the bay), is demonstrated well in Figures 32-34.

The backbarrier tide curves (Figs. 32-34) were recorded from a tide staff that was located in the middle of the

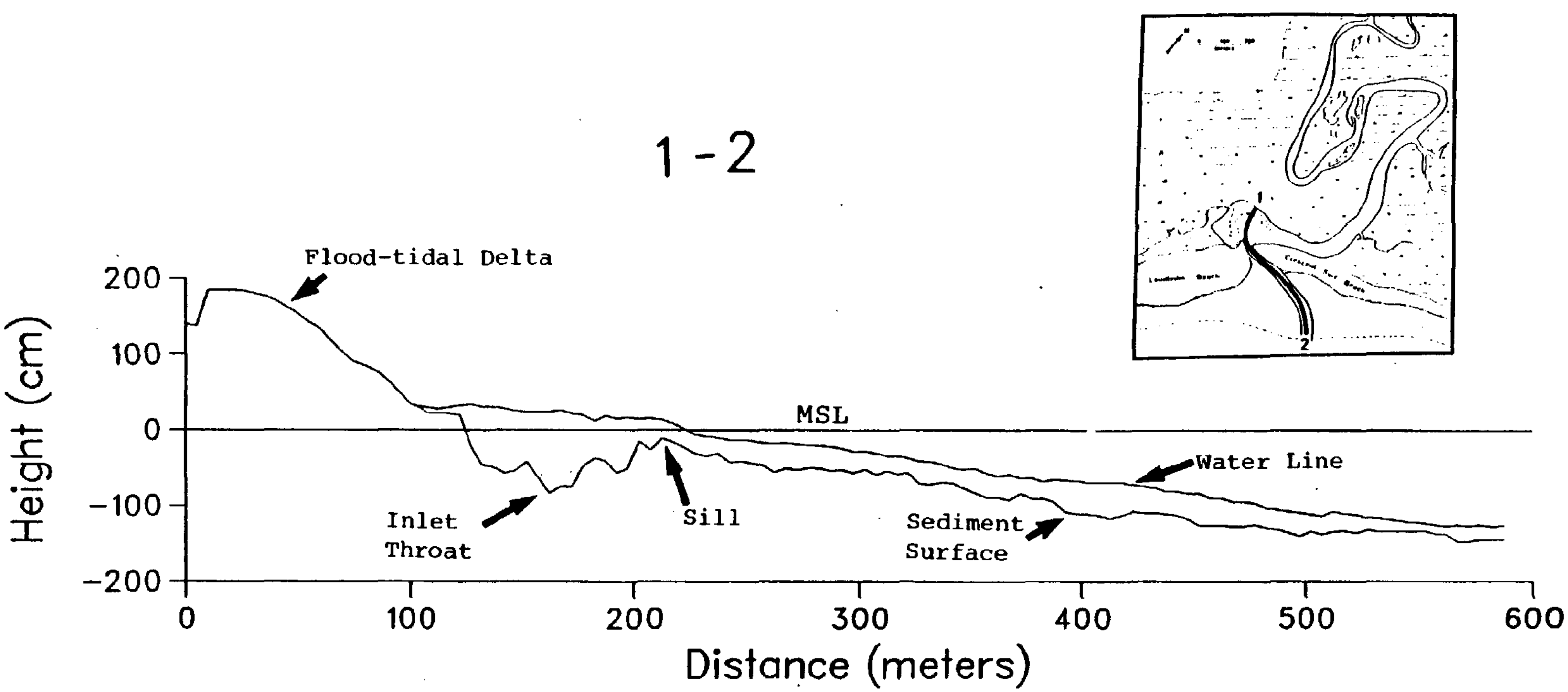


Figure 37. Longitudinal profile down the axis of Little River Inlet entrance channel from the flood-tidal delta to the low tide line. Notice the slope in the water line below the sill.

channel on the landward side of Crescent Surf Beach, 100 m from the inlet throat (see Fig. 31). The tide staff was kept in position during the entire field period. The reduction of the ocean tide through the inlet can be almost fully accounted for by the truncation of the tidal wave due to the gravel sill. It has been observed in the field that regardless of the elevation of the ocean low tide, there is always approximately .15 m of water that flows over the sill until the tide is reversed. With this knowledge the bay tidal range can be predicted by subtracting the height of the sill (1.21 m) plus the depth of water over the sill (.15 m) from the predicted high tide elevation of the ocean. This exercise has been performed in Table 3, indicating an average difference of 0.02 m between the predicted and recorded tidal ranges. It should be noted that during hydrography periods, meteorological tides were negligible. In addition it should be emphasized that low water in the bay always reaches the same elevation and therefore, bay tidal range is a function of ocean high tide level alone (Fig. 38).

The length of the ebb duration is controlled by tidal range, whereby larger tidal ranges produce longer ebb durations. A close correlation between these two parameters is seen in Table 1. The relationship is explained by the fact that as tidal range increases, the ocean tide has a

TABLE 3

Tidal Range Data

| Date | Tidal Stage | Predicted tide (1) levels (m) | Predicted High tide level(m)(PHT) | PHT-(2) 1.36m | Recorded (3) Tidal Range (m) | Difference between Predicted and Recorded |
|---|---|---|---|---|---|---|
| 8 July 1987 | Ebb | 2.5 - 0.2 | 2.5 | 1.14 | 1.13 | .01 |
| | Flood | 0.2 - 3.1 | 3.1 | 1.74 | 1.69 | .05 |
| 22 July 1987 | Ebb | 2.3 - 0.4 | 2.3 | .94 | .98 | -.04 |
| | Flood | 0.4 - 2.8 | 2.8 | 1.44 | 1.43 | .01 |
| 11-12 August 1987 | Ebb | 3.0 - ¯0.2 | 3.0 | 1.64 | 1.67 | ¯.03 |
| | Flood | ¯0.2 - 3.3 | 3.3 | 1.94 | 1.84 | .10 |
| | | | | | Average | .02 |

1. Predicted from NOAA (1987) Tide Tables for nearby Kennebunkport
2. 1.36 equals height of sill (1.21 m) above NLW plus depth of water over sill (.15 m)
3. Tidal range data from Table 1

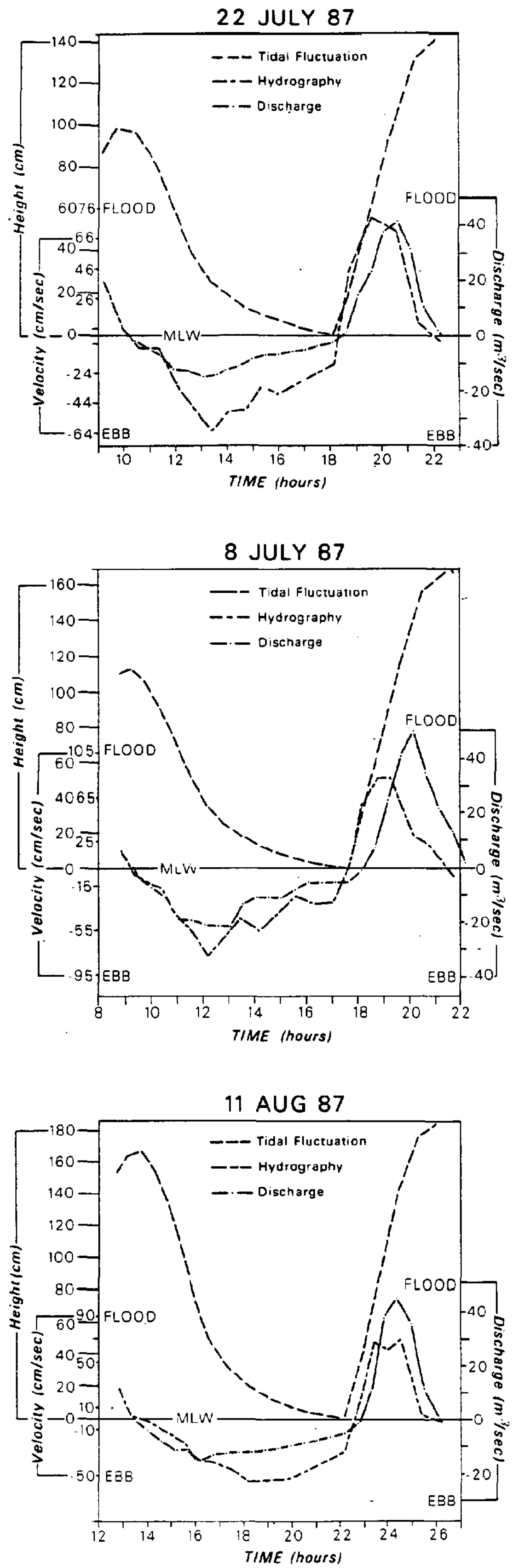


Figure 38. Plots of superimposed tide curve, current velocity, and discharge for spring, mean and neap tides.

greater distance to rise before overcoming the sill, and thus more flooding time required before a tide shift occurs inside the inlet (Fig. 39).

One interesting aspect of the tidal current data, that is not easily explained, is the inverse correlation that exists between tidal range and current strength. Normally, if the inlet channel dimensions do not change drastically at times of spring versus neap tidal conditions, then increasing tidal range (by increasing high tide elevation) at an inlet causes a larger tidal prism which requires stronger tidal currents. At Little River Inlet the opposite trend was often observed (ie. the strongest ebb velocities were recorded during neap tide conditions and conversely; Table 1; Figs. 35, 36, and 39). However, it should be recognized that this trend is based on only three data points and during one of the hydrographies a different current meter was used. Ongoing tidal current studies are aimed at documenting the factors controlling tidal current strength at the inlet.

## INLET STABILITY

The cross sectional area versus tidal prism equilibrium condition was evaluated for Little River Inlet using Jarrett's (1976) regression curves. Tidal prisms were

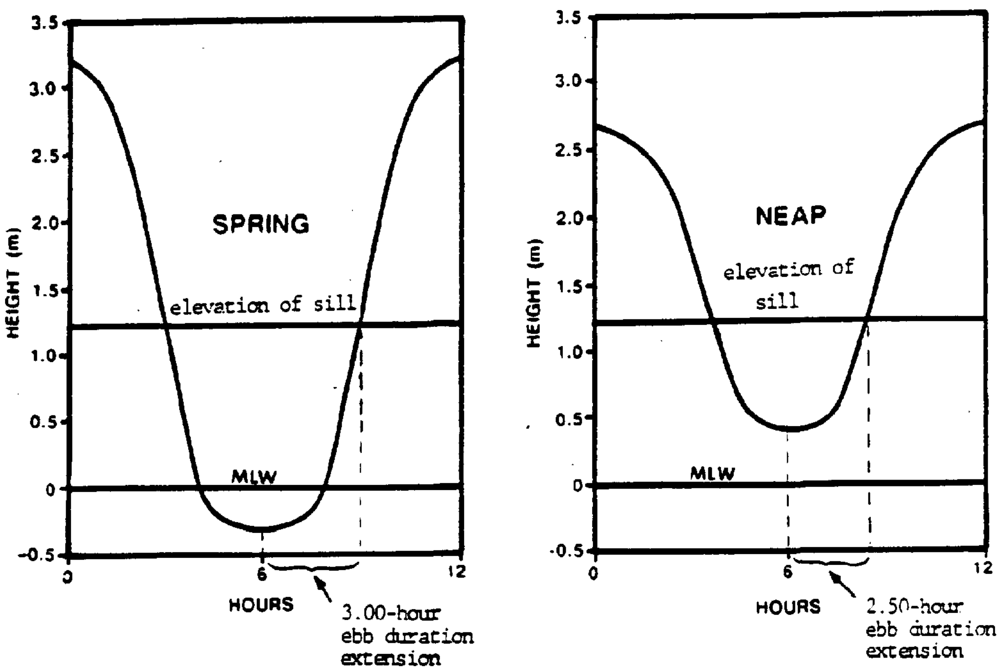


Figure 39. Plots of the elevation of the sill with respect to the spring and neap ocean tide curves. Lower tides result in longer ebb durations.

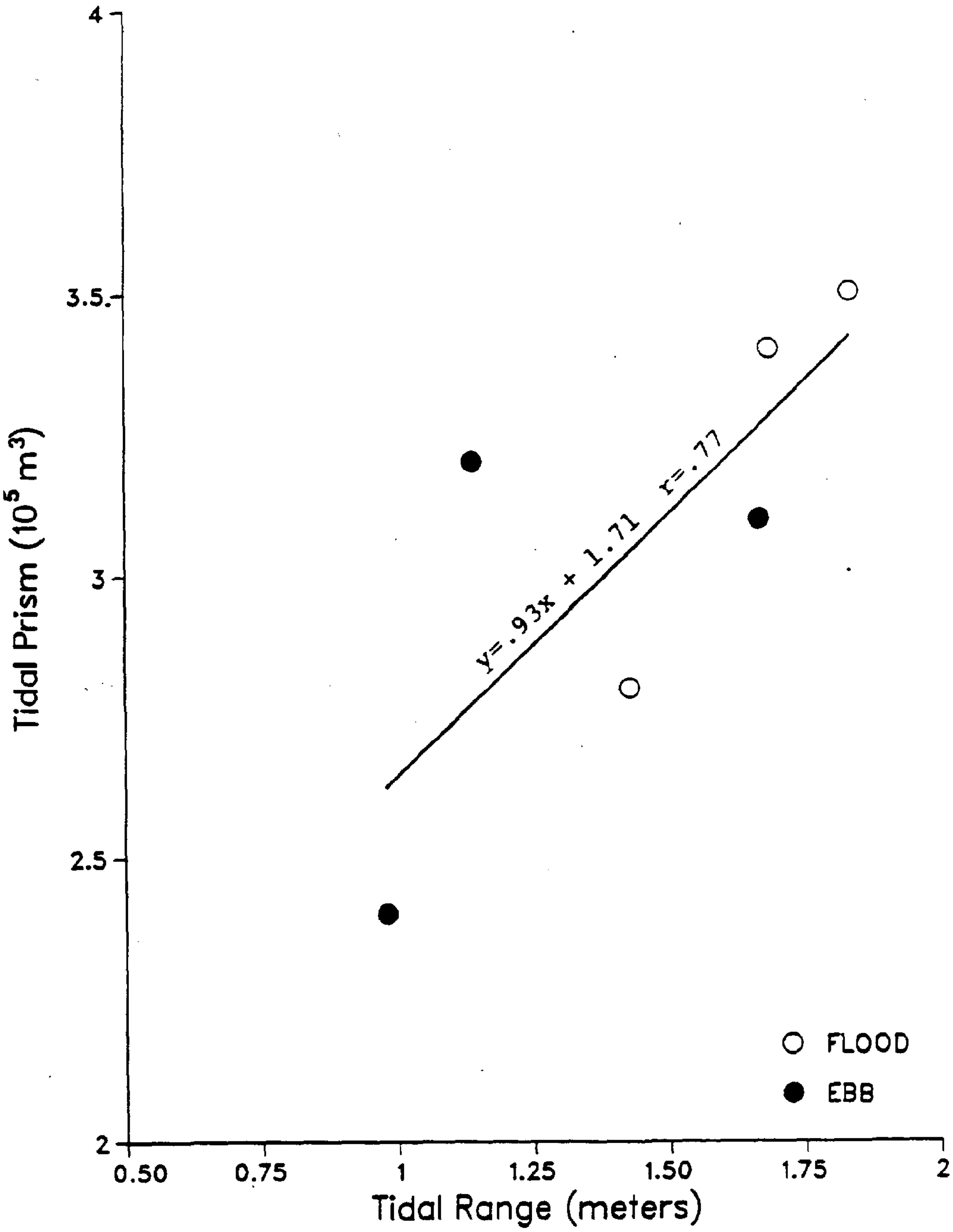


Figure 40. Plot of tidal prisms versus tidal range as determined from data collected at the inlet throat.

calculated for six half tidal cycles and then plotted against their respective tidal range (Fig. 40). The regression curve that was established from this relationship was used to determine the average spring tidal prism at the inlet ($3.2 \times 10^5$ $m^3$). Using Jarrett's (1976) equation for non-jettied inlets, the predicted equilibrium cross sectional area for Little River Inlet was 17 $m^2$ (Fig. 41). Although this area is 23% less than the measured cross section of 22 $m^2$ that was surveyed in October 1987, it is well within the 95% confidence of Jarrett's (1976) curve. It should also be noted that long-term monitoring of the inlet channel demonstrates that its cross sectional area varies by approximately 15 to 20% on a yearly basis.

## SAND TRANSPORT PATTERNS

Sand transport patterns at the inlet are inferred from tidal current data, bedform and sedimentological trends and the morphological history of the region. Of importance is the fact that the inlet is in equilibrium with its tidal prism and the historical records indicate that the inlet has maintained the same relative position with no net migrations during at least the past two centuries. These conditions would seem to suggest that most of the sediment at the inlet is recirculated and there are no long-term sediment sinks

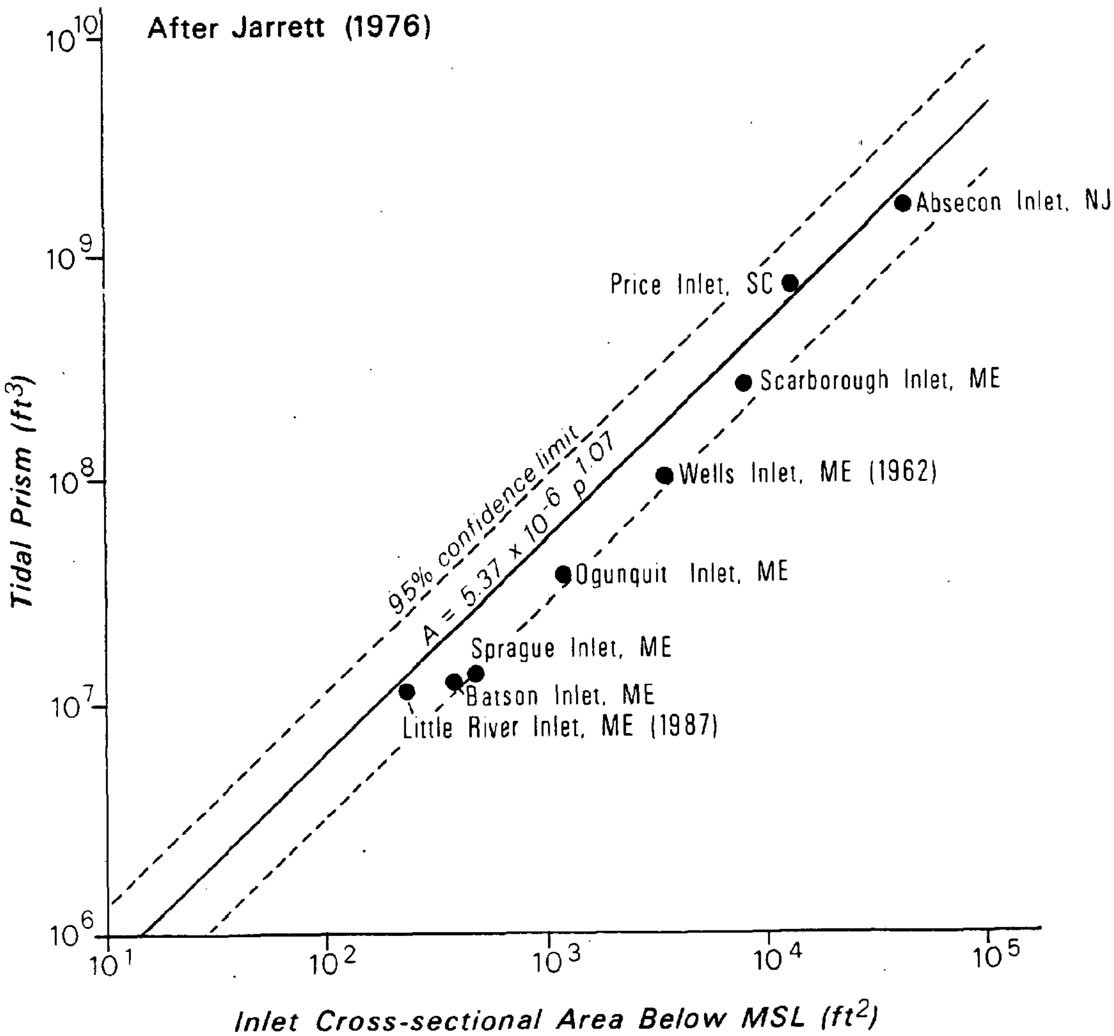


Figure 41. Jarrett's (1976) regression curve for tidal prism versus inlet cross sectional area for non-structured and one jetty inlets. Little River Inlet plots well within the 95% confidence limits of Jarrett's curve.

that would cause changes to the inlet hydraulics or general morphology of the system. This point is best demonstrated by considering the hypsometry of the backbarrier. As seen in Figure 4, the open-water area comprises only 10% of the entire backbarrier area and that these open-water areas are chiefly the tidal channels. Thus, if the inlet was truely a sediment sink, as indicated by the velocity data, then the backbarrier channels should be shoaling and the inlet should be gradually closing as its tidal prism was being reduced. The 1770 map of the Wells region (Fig. 16) shows that Little River Inlet was close in size and morphology as it appears today.

Perhaps a case could be made that during the past 200 years sand has been infilling the backbarrier channels, but that the rate of sedimentation has been compensated by sea level rise during the same period. There are historical data, including vertical aerial photographs spanning the last 49 years (Fig. 18), which indicate that intertidal areas close to the inlet, particularly the region behind Laudholm Beach, have been filling with sand. However, to fully document the long-term sand transport patterns at the inlet will require a more rigorous study including: 1. sand tracer experiments, 2. further investigation of the current regime, especially in the backbarrier tidal channels, 3. documentation of inlet processes during major storms, and finally, 4.vibra-coring of the marsh, intertidal flats and barrier spit systems. The latter investigation would be particularly useful in predicting future changes at the inlet in light of the predicted increase in the rate of sea level rise.

## CONCLUSIONS

1. The presence of Little River Inlet is due to the slight embayed nature of this section of the coast, which is related to the drainage of Branch Brook and the Merriland River. The barrier spits that border the inlet likely developed from sediment that was eroded from inland glacio-fluvial and glacio-marine deposits and transported to the coast following deglaciation via the Webhannet, Merriland, Branch Brook and Mousam River systems.

2. Despite the large size of its backbarrier, Little River Inlet has a small tidal prism and a small equilibrium channel cross section. This is because the bay is filled with Spartina marsh, a quality that is characteristic of many tidal inlets in Maine. The reason for the large percentage of the backbarrier at the supratidal elevation is not known; however, it may be related to a

high rate of peat production or the initial sedimentation history of the bay.

3. Historical information indicates that the inlet is relatively stable in its present location. Although it has changed positions through inlet migration and spit breaching processes these movements have been less than 200 m with no recorded net migration.

4. The inlet is dominated by flood tidal currents which resilt from a flood duration that is commonly more than 4 hours longer than the ebb duration. This asymmetry is caused by a truncation (1.36 m) of the ocean tidal wave by a gravel sill that is located 50 m seaward of the inlet throat. The reduced tidal ranges in the bay behind the inlet are fully explained by the truncation phenomenon.

## REFERENCES CITED


Belknap, D.F., Shipp, R.C., Kelley, J.T., and Schnitker, D., 1988, Depositional sequence modelling of late Quaternary geologic history: Sheepscot Bay, west-central Maine coast, in: Tucker, R.D., (ed.), C.T. Jackson Sesquicentennial Volume, Maine Geological Survey, Augusta, ME, p. 71-86.

Byrne, R.J., and Zeigler, J.M., 1977, Coastal Engineering Study, Well's Harbor , Maine, U.S. Army Corps. of Engineers.

Boyd, R., Bowen, A. J., and Hall, R. K., 1987, An evolutionary model for transgressive sedimentation on the Eastern Shore of Nova Scotia, in: FitzGerald, D. M., and Rosen, P. S. (eds.), Glaciated Coasts, Academic Press, San Diego, CA, p. 87-114.

D.Amore, D.W., 1983, Hydrogeology and Geomorphology of the Great Sanford Outwash Plain, York County, Maine, with particular emphasis on the Branch Brook Watershed; Ph.D. Dissertation, Boston University, 1983.

Farrell, S.C., Rhodes, E.G., and Colonell, J.M., 1971, Saco Bay, Maine: a test of computer models for wave forecasting and refraction, Geol. Soc. Amer., Abs. with Prog., v. 3, p. 562-563.

Fink, L.K., Jr., Fisher, N.A., and FitzGerald, D.M., 1984, Coastal Geomorphology of Ogunquit, Laudholm, Drake's Island, Well's Inlet, and Well's Beach, Southeastern Maine, in: Hansen, L., Geology of Southern New England, NEIGC, Dept. of Geological Sciences, Salem State College, Salem, MA, Part 18, p. 1-23.

Fink, L.K., Jr., Nelson, B.W., Fischer, N.A., Foster, R.G., and White, C.M., An atlas of Maine beaches: Maine State Planning Office Report, Office of Coastal Zone Management, Augusta, ME, (in press).

Folk, R.L., 1968, Petrology of Sedimentary Rocks, Univ. of Texas, University Station, Austin, TX, 170 p.

Garrett, C., 1972, Tidal resonance in the Bay of Fundy and Gulf of Maine, Nature, v. 238, p. 441-443.

Greenberg, D.A., 1979, A numerical model investigation of tidal phenomena in the Bay of Fundy and Gulf of Maine, Marine Geodesy, v. 2, p. 161-187.

Hayes, M.O., 1979, Barrier island morphology as a function of tidal and wave regime, in Leatherman, S.P., ed., Barrier Islands: From the Gulf of St. Lawrence to the Gulf of Mexico: New York, Academic Press, p. 1-28.

Hussey, A.M., II, 1959, Age of intertidal tree stumps at Wells Beach and Kennebunk Beach, Maine, reprint Jour. of Sed. Petr., p. 464-465.

Hussey, A.M., II, 1970, Observations on the origin and development of the Wells Beach Area, Maine, Maine Geol. Survey, Bulletin 23, p. 58-68.

Jarrett, J.T., 1976, Tidal prism-inlet are relationships, G.I.T.I. Report #3, Dept. of the Army, Corps. of Engineers, Waterways Experiment Station, Vicksburg, MS.

Jensen, X.E., 1983, Atlantic Coast hindcasting shallow water significant wave information, WIS Report #8, Vicksburg, MS, 75 p.

Kelley, J.T., Kelley, A.R., Belknap, D.F., and Ship, R.C., 1986, Variability in the evolution of two adjacent bedrock-framed estuaries in Maine, in Wolfe, D., (ed.), Estuarine Variability, Academic Press, New York, p. 21-42.

Lincoln, J.M., and FitzGerald, D.M., 1988, Tidal distortions and flood dominance at five small inlets in Southern Maine, Marine Geology, (in press).

McIntire, W.G., and Morgan, J.P., 1963, Recent geomorphic history of Plum Island, MA and adjacent coasts, Louisiana State Univ. Studies, Coastal Studies Series #8, 44 p.

Nelson, B.W., 1979, Shoreline changes and physiography of Maine's sandy coastal beaches, unpubl. Master's Thesis, Dept. of Ocn., Univ. of Maine, Orono, Maine, 302 p.

Nelson, B.W., and Fink, L.K., Jr., 1978, Geological and botanical features of sand beach systems in Maine. Critical Areas Program, Maine State Planning Office, Augusta, ME, 269 p.

Nummedal, D., and Fisher, I., 1978, Process-response models for depositional shorelines: the German and Georgia Bights, Amer. Soc. of Civil Engr., Proc. 16th Coastal Engr. Conf., p. 1215-1231.

Redfield, A.C., 1980, Introduction to Tides, Marine Science International, Woods Hole, MA, 108 p.

Richardson, W.S., 1977, Forecasting beach erosion along the oceanic Thesis, School of Marine Science, College of William and Mary, Williamsburg, VA, 121 p.

Smith, G.W., 1980, End Moraine and Glaciofluvial Deposits: Cumberland and York Counties, ME, Maine Geological Survey, Augusta, ME.

Timson, B.S., 1977, A Handbook of Coastal Marine Geological Environments of the Maine Coast, Maine Dept. of Conservation and Maine State Planning Office, Augusta, ME.

Timson, B.S., and Kale, D., 1976, Historical changes of the Webhannet River Inlet, Report to the New England Division, U.S. Army, Corps. of Engr.

U.S. Army Corps. of Engineers, 1957, Saco, Maine Beach Erosion Control Study, House Document #32, 85th Congress, 1st Session, 37 p.